100 *Organometallics* **2011,** *30,* 100–114
DOI: 10.1021/om100827z

ORGANOMETALLICS
Article

Synthesis, Characterization, Interionic Structure, and Self-Aggregation Tendency of Zirconaaziridinium Salts Bearing Long Alkyl Chains

Luca Rocchigiani, Gianfranco Bellachioma, Gianluca Ciancaleoni, Alceo Macchioni,* Daniele Zuccaccia, and Cristiano Zuccaccia*

Dipartimento di Chimica, Università degli Studi di Perugia, via Elce di Sotto 8, I-06123 Perugia, Italy

Received August 25, 2010

Zirconaaziridinium inner sphere ion pairs (ISIPs) bearing alkyl chains of different lengths, $[Cp_2Zr(\eta^2\text{-}CH_2NR^1R^2)^+\cdots X^-]$ (R^1 = Me, $R^2 = C_2H_5$, $X^- = MeB(C_6F_5)_3^-$, **Zr^{NC2}BN**; R^1 = Me, $R^2 = C_{16}H_{33}$, $X^- = MeB(C_6F_5)_3^-$, **Zr^{NC16}BN**; $R^1 = R^2 = C_{18}H_{37}$, $X^- = MeB(C_6F_5)_3^-$, **Zr^{NC18}BN**; R^1 = Me, R^2 = Ph, $X^- = MeB(C_6F_5)_3^-$, **Zr^{NPh}BN**; $R^1 = R^2 = C_{18}H_{37}$, $X^- = B(C_6F_5)_4^-$, **Zr^{NC18}BT**; R^1 = Me, R^2 = Ph, $X^- = B(C_6F_5)_4^-$, **Zr^{NPh}BT**), have been synthesized by the reaction of $[Cp_2ZrMe^+\cdots MeB(C_6F_5)_3^-]$ or $[Cp_2ZrMe^+\cdots B(C_6F_5)_4^-]$ with the suitable tertiary amine followed by selective C−H activation of one Me group of the coordinated amine and methane elimination. Subsequent reaction of ISIPs with THF afforded the corresponding outer-sphere ion pairs (OSIPs) ([**Zr^{NC2}THF**][**BN**], [**Zr^{NC16}THF**][**BN**], [**Zr^{NC18}THF**][**BN**], [**Zr^{NPh}THF**][**BN**], [**Zr^{NC18}THF**][**BT**], [**Zr^{NPh}THF**][**BT**]) in which the anion has been displaced into the second coordination sphere. The interionic structure in solution (i.e., the relative cation−anion position) and the self-aggregation level of both ISIPs and OSIPs have been investigated by means of ^{1}H NOESY, ^{19}F,^{1}H HOESY, and diffusion PGSE NMR methods, in low polar solvents. It is found that, independent of the nature or length of the alkyl chains, the anion prefers to pair with the cation from the side of the nitrogen atom and THF in ISIPs and OSIPs, respectively. Self-aggregation of ion pairs into higher aggregates is also weakly influenced by the nature of the alkyl chains, but it is strictly connected with the nature of the counterion: ISIPs and OSIPs bearing $B(C_6F_5)_4^-$ showed an increased tendency to form higher aggregates with respect to those containing $MeB(C_6F_5)_3^-$. The level of the self-aggregation in benzene-d_6 and cyclohexane-d_{12} has been quantified by fitting the hydrodynamic volumes obtained from NMR diffusion experiments with several models of indefinite self-association. The IK model, in which the equilibrium constants slightly increase on increasing the aggregation step, best describes the experimental trends in all cases. The standard Gibbs free energy of self-association at 297 K (ΔG^0) for **Zr^{NC18}BN** is -6.7 ± 0.2 kJ mol^{-1} and -12.6 ± 0.7 kJ mol^{-1} in benzene-d_6 and cyclohexane-d_{12}, respectively. In the same solvents, the values of ΔG^0 are -17.9 ± 0.5 kJ mol^{-1} and -25.0 ± 0.3 kJ mol^{-1} for [**Zr^{NC18}THF**][**BT**]. At room temperature, 80% and 4% of [**Zr^{NC18}THF**][**BT**] are present in the form of ion pairs in cyclohexane-d_{12} at analytical concentrations of 10^{-5} and 10^{-3} M, respectively. The self-aggregation of [**Zr^{NC18}THF**][**BN**] in cyclohexane-d_{12} is strongly depressed by increasing the temperature.

Introduction

It is generally accepted that $[Cp_2MR^+\cdots X^-]$ metallocenium ion pairs are the active catalysts in homogeneous Ziegler−Natta olefin polymerization.[1] The strength of the cation−anion interaction in these ion pairs is of great importance for the activity, stability, and selectivity of the catalytic system[2] because the nature of the anion may profoundly alter the relative rates of the elementary catalytic steps.[3] Since the ion pair symmetrization process (i.e., the process that exchanges the anion from one side of the zirconocenium cation to the other) is sensitive to the strength of the cation−anion interaction, the dynamic of ion pair symmetrization has been extensively studied by NMR methods, in an attempt to correlate anion mobility with catalytic

*To whom correspondence should be addressed. E-mail: cristiano.zuccaccia@unipg.it.

(1) (a) Gibson, V. C.; Spitzmesser, S. K. *Chem. Rev.* **2003**, *103*, 283. (b) Pedeutour, J.-N.; Radhakrishnan, K.; Cramail, H.; Deffieux, A. *Macromol. Rapid Commun.* **2001**, *22*, 1095. (c) Gladysz, J. A., Ed. *Chem. Rev.* **2000**, *100* (special issue on "Frontiers in Metal-Catalyzed Polymerization"). (d) Marks, T. J., Stevens, J. C., Eds. *Top. Catal.* **1999**, *15* and references therein. (e) Britovsek, G. J. P.; Gibson, V. C.; Wass, D. F. *Angew. Chem., Int. Ed.* **1999**, *38*, 428. (f) Kaminsky, W.; Arndt, M. *Adv. Polym. Sci.* **1997**, *127*, 144. (g) Bochmann, M. *J. Chem. Soc., Dalton Trans.* **1996**, 255. (h) Brintzinger, H. H.; Fischer, D.; Mülhaupt, R..; Rieger, B.; Waymouth, R. *Angew. Chem., Int. Ed. Engl.* **1995**, *34*, 1143.

(2) (a) Chen, E. Y. X.; Marks, T. J. *Chem. Rev.* **2000**, *100*, 1391. (b) Bochmann, M. *J. Organomet. Chem.* **2004**, *689*, 3982.

(3) (a) Chen, M.-C.; Roberts, J. A.; Marks, T. J. *J. Am. Chem. Soc.* **2004**, *126*, 4605and references therein. (b) Roberts, J. A. S.; Chen, M.-C.; Seyam, A. M.; Li, L.; Zuccaccia, C.; Stahl, N. G.; Marks, T. J. *J. Am. Chem. Soc.* **2007**, *129*, 12713.

 Published on Web 12/14/2010

performances.[4] In particular, the experimental observations that an increased metallocenium concentration or addition of an external salt caused an entropic acceleration of the ion pair symmetrization process led Brintzinger and co-workers[5] to propose that ionic aggregates larger than ion pairs can be formed in appreciable amounts under catalytic conditions and may take part in the polymerization process.[6] The latter hypothesis was further reinforced by diffusion NMR experiments, which showed the formation of ion quadruples from zirconocenium ion pairs in benzene-d_6 at concentrations around 10^{-3} M.[7] Successively, in collaboration with Marks and co-workers, we demonstrated that ion pairs bearing weakly coordinating anions, such as $MeB(C_6F_5)_3^-$ and $FAl[2\text{-}(C_6F_5)(C_6F_4)]_3^-$, in the first coordination sphere (ISIPs = inner-sphere ion pairs)[8] exhibit a negligible tendency to self-associate in benzene-d_6.[9] In contrast, ion pairs in which the counterion resides in the second coordination sphere (OSIPs = outer-sphere ion pairs)[8] showed a marked tendency to self-aggregate, but a negligible percentage of higher aggregates are generated at catalytic concentration values ($< 10^{-4}$ M) in benzene-d_6.[10] In general, it seems that the higher the charge separation in the ion pairs, the higher their tendency to form higher aggregates.[11] Thus, if the search for large counteranions with a dispersed charge, which are less and less coordinating,[12] reduces the possibility that the anion competes with the substrate for the coordination at the metal, on the one hand, it increases the charge separation and the possibility of forming larger aggregates. Clearly, also an enhanced dimension of the cation[13] may contribute to reduce the ion-pair strength, thereby increasing the charge separation and the tendency to self-aggregate. In this respect, it should be noted that, during the polymerization process, a rapid growth of the polymer chain in the proximity of the catalytic site necessarily occurs. Consequently, the enhanced dimension of the cation in the active species may lead to an increase of ion pair separation and self-aggregation tendency. For example, an increase of the dipole moment as a function of the isotactic propylene chain length, in a silicon-bridged zirconocene ion pair, was predicted by Klesing and Bettonville through DFT (density functional theory) calculations.[14] An additional layer of complexity is faced when solvents with relative permittivity (ε_r) lower than that of benzene are taken into account. These solvents, as hexanes or isoparaffins, are by far the most used reaction media in industrial applications, but structural and dynamic investigations of ion pairs in these solvents are particularly challenging.[15] With the goal of obtaining information about the position of the counterion during the growth of the polymer chain and the tendency of ion pairs bearing a polymer chain to self-aggregate, we decided to synthesize model zirconocenium ion pairs with alkylic chains of different length and investigate them through advanced NMR techniques.[16] We focused on two commonly used anions, namely $MeB(C_6F_5)_3^-$[17] and $B(C_6F_5)_4^-$,[18] which are representative of weakly and very weakly coordinating anions, respectively. In the absence of a stabilizing donor ligand, $MeB(C_6F_5)_3^-$ is usually found to form loosely associated ISIPs with highly electrophilic early-transition-metal centers by way of M−Me agostic interactions.[2] More recently it has been observed that the $MeB(C_6F_5)_3^-$ may also form OSIPs in the absence of a nucleophile.[19] The presence of long alkyl chains on the cation rendered zirconocenium ion pairs soluble in cyclohexane, providing us the unique possibility to explore their self-aggregation tendency in a reaction medium with characteristics very similar to those used in industrial plants.

The Results and Discussion section of the paper is divided into three parts. First, a description of the synthesis and characterization in solution of the ion pairs, from both the intramolecular and interionic points of view, is presented. Second, a detailed examination of the self-aggregation behavior is discussed. Finally, a quantitative analysis of the self-aggregation process, including relevant thermodynamic parameters and catalyst speciation in terms of ion pairs or higher order aggregates, is offered. When possible, the experimental results based on NMR are contrasted and analyzed with respect to the outcome of DFT calculations.

Results and Discussion

1. Synthesis and Characterization of Zirconaaziridinium Ion Pairs. Schemes 1 and 2 illustrate the strategy for the synthesis of zirconaaziridinium ion pairs, which incorporate alkyl chains of different length into the cation. The initial step of the synthesis is the methide abstraction (or protonolysis) from the complex Cp_2ZrMe_2 ($\mathbf{Zr^{Me_2}}$, Cp = cyclopentadienyl anion) using a suitable Lewis ($B(C_6F_5)_3$ and $CPh_3^+B(C_6F_5)_4^-$) or Brønsted ($HN(Me)_2Ph^+B(C_6F_5)_4^-$) acid. This leads to $[Cp_2ZrMe^+\cdots MeB(C_6F_5)_3^-]$ ($\mathbf{Zr^{Me}BN}$, $\mathbf{BN^-}$ = $MeB(C_6F_5)_3^-$)[17a] and $[Cp_2ZrMe^+\cdots B(C_6F_5)_4^-]$ ($\mathbf{Zr^{Me}BT}$, $\mathbf{BT^-}$ = $B(C_6F_5)_4^-$) ISIPs.[20] The latter are treated

(4) For a few examples see: (a) Yang, X.; Stern, C. L.; Marks, T. J. *J. Am. Chem. Soc.* **1991**, *113*, 3623. (b) Siedle, A. R.; Newmark, R. A. *J. Organomet. Chem.* **1995**, *497*, 119. (c) Deck, P. A.; Beswick, C. L.; Marks, T. J. *J. Am. Chem. Soc.* **1998**, *120*, 1772. (d) Jia, L.; Yang, X.; Stern, C. L.; Marks, T. J. *Organometallics* **1997**, *16*, 842. (e) Mohammed, M.; Nele, M.; Al-Humydi, A.; Xin, S.; Stapleton, R. A.; Collins, S. *J. Am. Chem. Soc.* **2003**, *125*, 7930. (f) Song, F.; Lancaster, S. J.; Cannon, R. D.; Schormann, M.; Humphrey, S. M.; Zuccaccia, C.; Macchioni, A.; Bochmann, M. *Organometallics* **2005**, *24*, 1315. (g) Alonso-Moreno, C.; Lancaster, S. J.; Zuccaccia, C.; Macchioni, A.; Bochmann, M. *J. Am. Chem. Soc.* **2007**, *129*, 9282. (h) Alonso-Moreno, C.; Lancaster, S. J.; Wright, J. A.; Hughes, D. L.; Zuccaccia, C.; Correa, A.; Macchioni, A.; Cavallo, L.; Bochmann, M. *Organometallics* **2008**, *27*, 5474.

(5) Beck, S.; Lieber, S.; Schaper, F.; Geyer, A.; Brintzinger, H. H. *J. Am. Chem. Soc.* **2001**, *123*, 1483.

(6) (a) Song, F.; Cannon, R. D.; Bochmann, M. *J. Am. Chem. Soc.* **2003**, *125*, 7641. (b) Song, F.; Cannon, R. D.; Lancaster, S. J.; Bochmann, M. *J. Mol. Catal. A* **2004**, *218*, 21.

(7) Beck, S.; Geyer, A.; Brintzinger, H. H. *Chem. Commun.* **1999**, 2477.

(8) Macchioni, A. *Chem. Rev.* **2005**, *105*, 2039.

(9) Stahl, N. G.; Zuccaccia, C.; Jensen, T. R.; Marks, T. J. *J. Am. Chem. Soc.* **2003**, *125*, 5256.

(10) Zuccaccia, C.; Stahl, N. G.; Macchioni, A.; Chen, M.-C.; Roberts, J. A.; Marks, T. J. *J. Am. Chem. Soc.* **2004**, *126*, 1448.

(11) (a) Zuccaccia, D.; Bellachioma, G.; Cardaci, G.; Ciancaleoni, G.; Zuccaccia, C.; Clot, E.; Macchioni, A. *Organometallics* **2007**, *26*, 3930. (b) Bellachioma, G.; Ciancaleoni, G.; Zuccaccia, C.; Zuccaccia, D.; Macchioni, A. *Coord. Chem. Rev.* **2008**, *252*, 2224.

(12) Krossing, I.; Raabe, I. *Angew. Chem., Int. Ed.* **2004**, *43*, 2066and references therein.

(13) Price, C. J.; Chen, H.-Y.; Launer, L. M.; Miller, S. A. *Angew. Chem., Int. Ed.* **2009**, *48*, 956.

(14) Klesing, A.; Bettonville, S. *Phys. Chem. Chem. Phys.* **1999**, *1*, 2373.

(15) (a) Beswick, C. L.; Marks, T. J. *Organometallics* **1999**, *18*, 2410. (b) Beswick, C. L.; Marks, T. J. *J. Am. Chem. Soc.* **2000**, *122*, 10358.

(16) Rocchigiani, L.; Zuccaccia, C.; Zuccaccia, D.; Macchioni, A. *Chem. Eur. J.* **2008**, *14*, 6589.

(17) Yang, X.; Stern, C. L.; Marks, T. J. *J. Am. Chem. Soc.* **1994**, *116*, 10015.

(18) Chien, J. C. W.; Tsai, W.-M.; Rausch, M. D. *J. Am. Chem. Soc.* **1991**, *113*, 8570.

(19) Ciancaleoni, G.; Fraldi, N.; Budzelaar, P. H. M.; Busico, V.; Macchioni, A. *Dalton Trans.* **2009**, *41*, 8824.

Scheme 1. Syntheses of ISIPs[a]

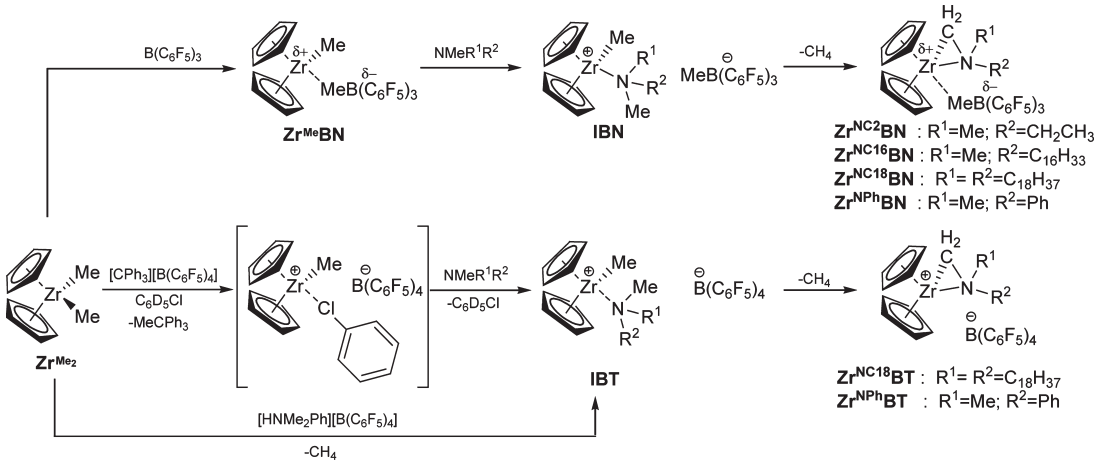

[a] Unless otherwise stated, the syntheses were performed in benzene-d_6.

Scheme 2. Syntheses of OSIPs

[Zr^NC2THF][BN]:R1=Me;R2=CH2CH3;X=BN
[Zr^NC16THF][BN]:R1=Me;R2=C16H33;X=BN
[Zr^NC18THF][BN]:R1= R2=C18H37;X=BN
[Zr^NPhTHF][BN]:R1=Me;R2=Ph;X=BN
[Zr^NC18THF][BT]:R1=R2=C18H37;X=BT
[Zr^NPhTHF][BT]:R1=Me;R2=Ph;X=BT

with 1 equiv of the suitable tertiary amine $NMeR^1R^2$ (R^1 = Me, R^2 = Et (**NC2**); R^1 = Me, $R^2 = C_{16}H_{33}$ (**NC16**); R^1 = $R^2 = C_{18}H_{37}$ (**NC18**); R^1 = Me, R^2 = Ph (**NPh**)) to afford the intermediates **IBN** and **IBT** OSIPs (Scheme 1), where the amine is coordinated to the metal center via the nitrogen lone pair.[21] At room temperature, **IBN** and **IBT** spontaneously transform into the final ISIPs by selective C−H activation of one methyl group on the tertiary amine and methane elimination.[22] The full course of the reaction was followed by NMR in the case of the reaction of **Zr^MeBN** with **NC16**. The displacement of the anion into the second coordination sphere is established by the small difference in chemical shift value between *m*-F and *p*-F resonances in the ^{19}F NMR spectrum ($\Delta\delta(m,p\text{-F}) = 2.9$ ppm).[23] Amine coordination in **IBN** is indicated by the low-frequency shift of the resonance due to the N−Me group(s) in both ^{1}H and ^{13}C NMR spectra.[24]

The disappearance of **IBN** and formation of the final product are accompanied by the release of CH_4 (δ_H 0.15 ppm). The reaction is complete in a few hours at room temperature. All the NMR data of the final complex are consistent with the general formula $[Cp_2Zr(\eta^2\text{-}CH_2NMeC_{16}H_{33})^+\cdots MeB(C_6F_5)_3^-]$ (**Zr^NC16BN**; Scheme 1).[25] In the complex **Zr^NC16BN** the resonances due to Cp rings (δ_H 5.26 and 5.24 ppm) and methylene hydrogen atoms of both the N−CH_2−R (δ_H 2.43 and 2.04 ppm) and Zr−CH_2−N groups (δ_H 1.68 and 1.37 ppm, $^2J_{HH}$ = 8.4 Hz) are not magnetically equivalent. These observations indicate a slow nitrogen inversion process on the ^{1}H NMR time scale.[26] Reasonably, this is due to the interaction between the nitrogen lone pair and the acidic zirconium center, which in principle may be intramolecular or intermolecular. The two possibilities are discriminated by analyzing the values of $^1J_{CH}$ coupling constants relative to the carbon atoms in α-positions with respect to the nitrogen. The ^{13}C NMR resonance of the Zr−CH_2−N moiety is observed at 55.4 ppm, while the related $^1J_{CH}$ coupling constant amounts to 150.3 Hz. This value is about 13 Hz larger than those observed for the N−CH_3 ($^1J_{CH}$ = 137.4 Hz) and N−CH_2−R ($^1J_{CH}$ = 137.2 Hz) groups and is diagnostic[27]

(20) The activation using $CPh_3^+B(C_6F_5)_4^-$ was carried out in chlorobenzene, a weakly coordinating solvent, to afford the intermediate $[Cp_2ZrMe(Cl\text{-}C_6H_5)^+\cdots B(C_6F_5)_4^-]$ (**Zr^Me(solv)BT**): Wu, F.; Dash, A. K.; Jordan, R. F. *J. Am. Chem. Soc.* **2004**, *126*, 15360.

(21) Schaper, F.; Geyer, A.; Brintzinger, H. H. *Organometallics* **2002**, *21*, 473.

(22) (a) Turner, H. W.; Hlatky, G. G.; Eckman, R. R. U.S. Patent 5,198,401, 1993. (b) Bertuleit, A.; Fritze, C.; Erker, G.; Fröhlich, R. *Organometallics* **1997**, *16*, 2891. (c) Wrobel, O.; Schaper, F.; Wieser, U.; Gregorius, H.; Brintzinger, H. H. *Organometallics* **2003**, *22*, 1320.

(23) The value of $\Delta\delta(m,p\text{-F})$ (^{19}F NMR) is a good probe of coordination of $MeB(C_6F_5)_3^-$ to cationic d^0 metals (values of 3−6 ppm indicate coordination; < 3 ppm indicates noncoordination). See: Horton, A. D.; de With, J. *Organometallics* **1997**, *16*, 5424and references therein.

(24) Wilson, P. A.; Wright, J. A.; Oganesyan, V. S.; Lancaster, S. J.; Bochmann, M. *Organometallics* **2008**, *27*, 6371and references therein.

(25) For other examples of metalla-aza-cyclopropanes see: (a) Dreos, R.; Felluga, A.; Nardin, G.; Randaccio, L.; Tauzher, G. *Organometallics* **2003**, *22*, 2486and references therein. (b) Hartshorn, R. M.; Telfer, S. G. *Dalton Trans.* **2000**, 2801. (c) Tonei, D. M.; Baker, L.-J.; Brothers, P. J.; Clark, G. R.; Ware, D. C. *Chem. Commun.* **1998**, 2593. (d) Marzilli, L. G.; Polson, S. M.; Hansen, L.; Moore, S. J.; Marzilli, P. A. *Inorg. Chem.* **1997**, *36*, 3854. (e) Lu, C. C.; Peters, J. C. *J. Am. Chem. Soc.* **2004**, *126*, 15818. (f) Maire, P.; Sreekanth, A.; Büttner, T.; Harmer, J.; Gromov, I.; Rüegger, H.; Breher, F.; Schweiger, A.; Grützmacher, H. *Angew. Chem., Int. Ed.* **2006**, *45*, 3265. (g) Adams, R. D.; Babin, J. E.; Kim, H.-S. *Organometallics* **1987**, *6*, 749. (h) Booij, M.; Kiers, N. H.; Meetsma, A.; Teuben, J. H. *Organometallics* **1989**, *8*, 2454. (i) Abbenhuis, H. C.L.; Feiken, N.; Haarman, H. F.; Grove, D. M.; Horn, E.; Spek, A. L.; Pfeffer, M.; van Koten, G. *Organometallics* **1993**, *12*, 2227. (j) Liu, G.; Beetstra, D. J.; Meetsma, A.; Hessen, B. *Organometallics* **2004**, *23*, 3914. (k) Knight, P. D.; Munslow, I.; O'Shaughnessy, P. N.; Scott, P. *Chem. Commun.* **2004**, 894. (l) Rankin, M. A.; McDonald, R.; Ferguson, M. J.; Stradiotto, M. *Organometallics* **2005**, *24*, 4981. (m) Liptau, P.; Carmona, D.; Oro, L. A.; Lahoz, F. J.; Kehr, G.; Erker, G. *Eur. J. Inorg. Chem.* **2004**, 4586. (n) Krut'ko, D. M.; Borzov, M. V.; Kirsanov, R. S.; Churakov, A. V.; Kuz'mina, L. G. *J. Organomet. Chem.* **2005**, *690*, 3243.

(26) Belostoskii, A. M.; Aped, P.; Hassner, A. *J. Mol. Struct. (THEOCHEM)* **1997**, *398−399*, 427–434.

(27) (a) Bertuleit, A.; Fritze, C.; Erker, G.; Fröhlich, R. *Organometallics* **1997**, *16*, 2891. (b) Pflug, J.; Bertuleit, A.; Kehr, G.; Fröhlich, R.; Erker, G. *Organometallics* **1999**, *16*, 3818. (c) Pflug, J.; Erker, G.; Kehr, G.; Fröhlich, R. *Eur. J. Inorg. Chem.* **2000**, 1795.

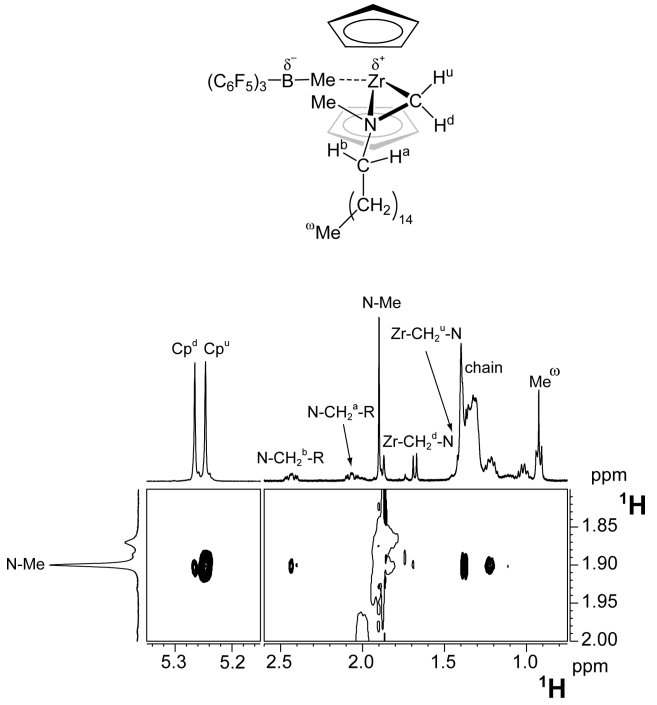

Figure 1. Two sections of the ^{1}H NOESY NMR spectrum of $\mathbf{Zr^{NC16}BN}$ (400.13 MHz, benzene-d_6, 297 K) showing the strong intramolecular interactions between the N−Me moiety and Zr−CH_2^u−N and Cp^u groups.

of the heterocyclopropane character of the zirconaaziridinium framework. In analogy with η^2-imine complexes of zirconium[28] two extreme resonance structures may in principle contribute to the description of the iminium−Zr bond, but that involving the π coordination of the iminium double bond to a formally Zr(II) center is certainly less important due to the high π basicity of Zr(II).[29] Full resonance assignment is easily accomplished by considering the plane defined by the azazirconacyclopropane ring (see Figure 1). For example, starting from the resonance due to the N−Me moiety (δ_H 1.90 ppm), the signals due to Zr−CH_2^u−N and Cp^u (arbitrarily we label as "up" (u) the groups that are positioned on the same side as the N−Me moiety with respect to the above-defined plane) are easily recognized by their intense NOE interaction with the N−Me group (Figure 1).

Having identified Zr−CH_2^u−N and Cp^u, the remaining resonances are assigned from the homo- and/or heteronuclear scalar and dipolar connectivities. The formation of the zirconaaziridinium metallacycle is accompanied by the reentering of the anion into the first coordination sphere of the cation. The chemical shift difference between *m*-F and *p*-F resonances is again used as a diagnostic tool. The $\Delta\delta(m,p\text{-F})$ observed in $\mathbf{Zr^{NC16}BN}$ amounts to 4.4 ppm, indicating that an ISIP is formed.[23] In agreement, the proton resonance due to B−Me appears at 0.07 ppm, a value which is about 1.3 ppm lower in frequency with respect to that observed for the "free" anion.[30] The same NMR arguments described above apply to all ion pairs containing the **BN** anion. However, for $\mathbf{Zr^{NC18}BN}$ the distinction between the "up" and "down" sides is no longer possible. As for the nature of cation−anion interaction in solution, the situation is more complicated in the case of complexes containing the **BT** anion, since no diagnostic tool has been reported that unambiguously allows us to discriminate between ISIPs and OSIPs.

Scheme 3

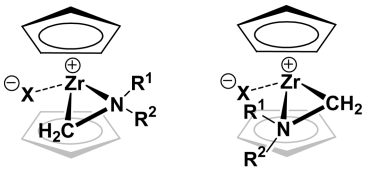

Addition of THF to the zirconaaziridinium ion pairs described above results in a fast and complete anion displacement, leading to the corresponding OSIPs as depicted in Scheme 2. Only one molecule of THF is incorporated into the cation even when a large excess of THF is used. The coordination of THF is indicated by the chemical shift values of the OCH_2 moiety. In particular, the proton resonance is observed around δ_H ~3.3−3.1 ppm, while the carbon resonance appears at δ_C ~78−77 ppm. These values are about 0.4 and 10 ppm lower and higher than in "free" THF, respectively.[31] The zirconaaziridinium skeleton remains intact, as demonstrated by the $^1J_{CH}$ value of the Zr−CH_2−N moiety (~154 Hz), while the anion displacement is clearly seen for ion pairs containing the **BN** anion by a decrease of the $\Delta\delta(m,p\text{-F})$ values.

2. Structure in Solution of ISIPs and OSIPs. Two structural arrangements are possible within the zirconaaziridinium cations described above: the *outside* structure with the carbon of the Zr−CH_2−N group interposed between the anion (or THF) and the nitrogen atom, and the *inside* structure with the nitrogen atom occupying the central position (Scheme 3).[32]

In solution, the two possibilities may be discriminated by means of homo- and heteronuclear NOE NMR measurements. For ISIPs containing the **BN** anion, strong dipolar interionic interactions are observed between B−Me and the *o*-F atoms of the anion and N−Me, N−CH_2−R, and both Cp moieties of the cation in ^{1}H NOESY and ^{19}F,^{1}H HOESY spectra. Figure 2 shows the case of $\mathbf{Zr^{NC16}BN}$ as an example. Interionic dipolar interactions are not observed for *m*-F and *p*-F nuclei, indicating that the anion is preferentially oriented in such a way that the B−Me group steadily points toward the cation.[10] Notably, we were unable to detect any interionic contacts involving the Zr−CH_2−N moiety, indicating that the *inside* structure is preferentially present in solution. Analogous results are obtained for all the ISIPs, including those containing the **BT** anion. In the latter case, interionic interactions involving the Cp(s), N−Me, and N−CH_2−R groups are observed for all the anion resonances, those due to *m*-F atoms being the strongest.

The *inside* coordination mode is also preferred for OSIPs, as demonstrated by the strong dipolar interactions present in

(28) Cummings, S. A.; Tunge, J. A.; Norton, J. R. *Top. Organomet. Chem.* **2005**, *10*, 1.

(29) Crabtree, R. H. *The Organometallic Chemistry of Transition Metals*; Wiley: New York, 2001.

(30) (a) Beck, S.; Prosenc, M. H.; Brintzinger, H.-H.; Goretzki, R.; Herfert, N.; Fink, G. *J. Mol. Catal. A: Chem.* **1996**, *111*, 67. (b) Beck, S.; Prosenc, M. H.; Brintzinger, H.-H. *J. Mol. Catal. A: Chem.* **1998**, *128*, 41.

(31) Gottlieb, H. E.; Kotlyar, V.; Nudelman, A. *J. Org. Chem.* **1997**, *62*, 7512.

(32) The *inside* and *outside* nomenclature was first introduced by: Tatsumi, K.; Nakamura, A.; Hofmann, P.; Staufert, P.; Hofmann, R. *J. Am. Chem. Soc.* **1985**, *107*, 4440.

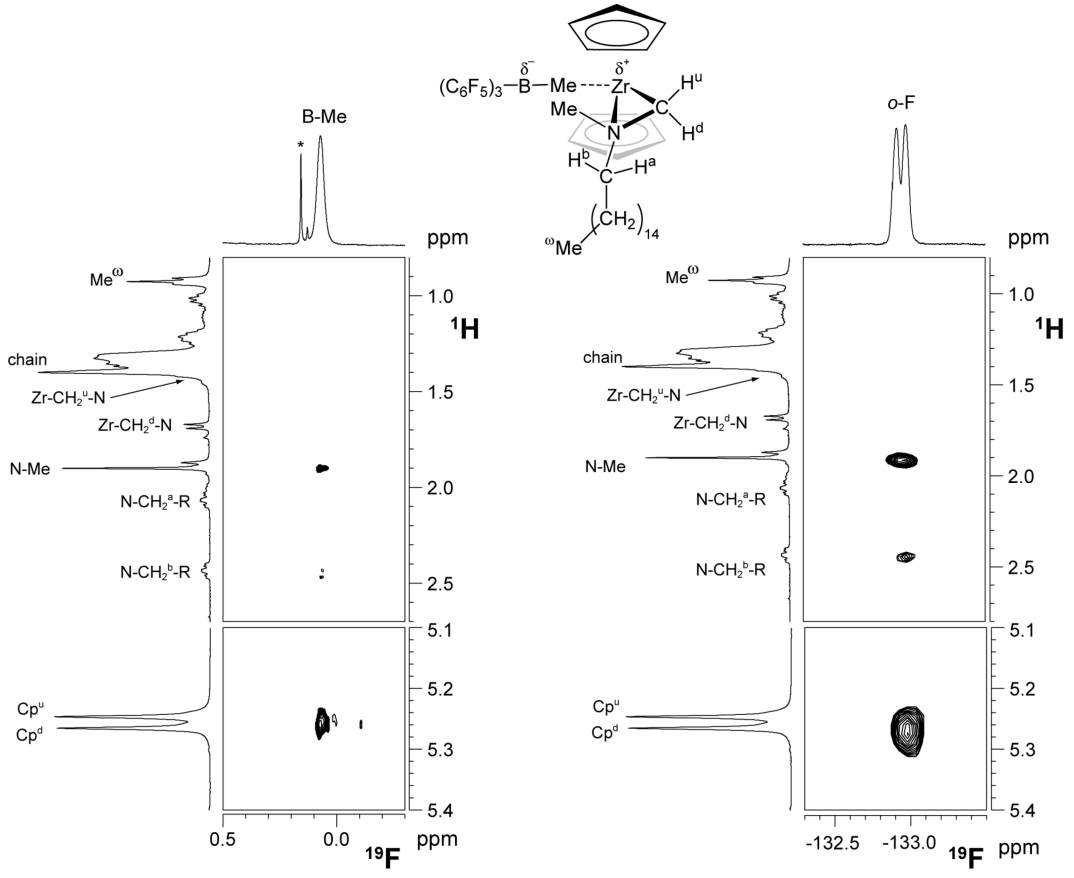

Figure 2. (left) Two sections of the ^{1}H NOESY NMR spectrum of $\mathbf{Zr^{NC16}BN}$ (400.13 MHz, benzene-d_6, 297 K) showing the interionic interactions between the B−Me moiety and N−Me, Cp^d, and Cp^u groups. (right) Two sections of the ^{19}F,^{1}H HOESY spectrum of $\mathbf{Zr^{NC16}BN}$ (376.47 MHz, benzene-d_6, 297 K) showing the interionic interactions between the fluorine atoms in ortho positions and the N−Me, Cp^d, Cp^u (strong), and N−CH$_2$−R (weak) groups. The spectra shown here refer to an in situ generation of $\mathbf{Zr^{NC16}BN}$ rather than to the purified complex. The asterisk denotes the resonance of CH_4. The small peak close to the B−Me resonance is due to an unknown impurity.

the ^{1}H NOESY spectrum between the O−CH$_2$ moiety of the coordinated THF and both the N−Me and N−CH$_2$−R groups. In agreement, dipolar contacts could not be detected between THF protons and the Zr−CH$_2$−N group.

In order to validate the conclusions based on NOE NMR measurements, we performed DFT quantum mechanical geometry optimizations for the *inside* and *outside* structures. Initially, the cation of [$\mathbf{Zr^{NC2}THF}$][**BN**] was optimized. The *inside* geometry ([$\mathbf{Zr^{NC2}THF}$]$^+_{inside}$) is about 7.5 kJ mol^{-1} more stable than the *outside* geometry ([$\mathbf{Zr^{NC2}THF}$]$^+_{outside}$). The higher stability of [$\mathbf{Zr^{NC2}THF}$]$^+_{inside}$ seems mainly due to steric factors, since the sterically demanding NMeEt moiety is oriented toward a relatively free region of the space, in front of the bent metallocene (Figure 3, top). In contrast, in [$\mathbf{Zr^{NC2}THF}$]$^+_{outside}$ the bulky NMeEt moiety is oriented toward a more hindered lateral position (Figure 3, bottom). To partially release such a steric congestion, the Cp rings adopt a quasi-eclipsed conformation and are partly tilted toward the side where the THF ligand is coordinated.

Similar considerations apply to the analysis of the *inside* and *outside* optimized geometries of $\mathbf{Zr^{NC2}BN}$ and $\mathbf{Zr^{NPh}BN}$. The *inside* geometry always is the most stable,[33] with the computed energy differences amounting to 23.8 and 41 kJ mol^{-1} for $\mathbf{Zr^{NC2}BN}$ and $\mathbf{Zr^{NPh}BN}$, respectively. The larger gap observed in the case of $\mathbf{Zr^{NPh}BN}$ most likely reflects the increased steric demand of the phenyl ring with respect to the ethyl group.

The interionic structures of OSIPs were investigated in solution by means of ^{1}H NOESY and ^{19}F,^{1}H HOESY NMR experiments. As an example, four relevant sections of the ^{19}F,^{1}H HOESY of [$\mathbf{Zr^{NC16}THF}$][**BN**] recorded in benzene-d_6 are shown in Figure 4.

In addition to the strong intramolecular NOE interaction between B−Me and *o*-F nuclei, NOE interionic interactions between *o*-F, *m*-F, and, in some cases, *p*-F nuclei and Cp, THF, and N−Me protons are observed. As in the case of the corresponding ISIPs, interionic contacts between the anion and Zr−CH$_2$−N are below detectability. Despite the overlap of the central CH$_2$ groups of the aliphatic chain with the protons of THF in β-positions, a careful quantification of the NOE contacts[34] indicates that they only weakly interact with the *o*-F and *m*-F nuclei of the counterion. These observations suggest that the counterion is prevalently located in front of

(33) The thermodynamic preference for the *inside* coordination mode seems rather general and independent from the nature of the additional donor ligand. For related zirconaaziridines see for example: (a) Buchwald, S. L.; Watson, B. T.; Wannamaker, M. W.; Dewan, J. C. *J. Am. Chem. Soc.* **1989**, *111*, 4486. (b) Gately, D. A.; Norton, J. R.; Goodson, P. A. *J. Am. Chem. Soc.* **1995**, *117*, 986. (c) Lubben, T. V.; Plössl, K.; Norton, J. R.; Miller, M. M.; Anderson, O. P. *Organometallics* **1992**, *11*, 122. On the other hand, cases have been reported where the ouside coordination geometry is observed in the solid state. See: (d) Cheung, M.-S.; Chan, H.-S.; Xie, Z. *Organometallics* **2005**, *24*, 5217.

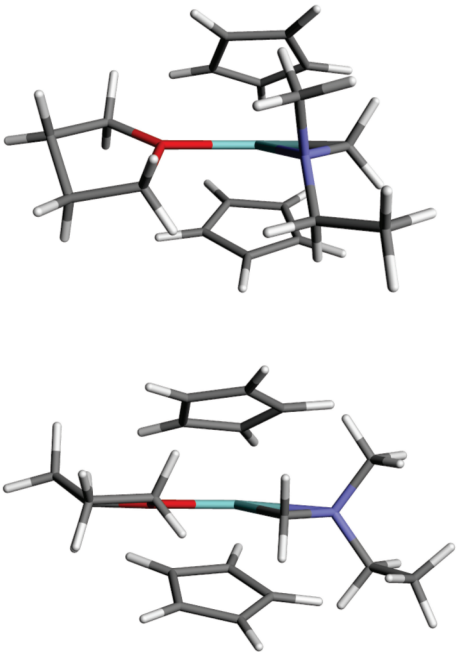

Figure 3. Optimized geometries of *inside* (top) and *outside* (bottom) structures of the $[\mathbf{Zr^{NC2}THF}]^+$ cation.

the cation, partially shifted toward the side of THF. As for the anion orientation, NOE quantification[34] carried out on the complex $[\mathbf{Zr^{NPh}THF}][\mathbf{BN}]$ indicates that the average interionic distance between the B−Me moiety of the anion and the α-THF protons of the cation is about 4.1 Å. In agreement with previous results,[10,35] this relatively large average interionic distance indicates that the orientation in which the B−Me moiety of the **BN** anion points away from the metal center is favored. Similar interionic interactions are observed for OSIPs containing the **BT** anion, indicating that the interionic structures of all the OSIPs are the same, independent of the nature of the R substituents on the nitrogen atom and the nature of the counterion.

The conclusions from NMR studies are in good agreement with the results of DFT calculations carried out on $[\mathbf{Zr^{NC2}THF}][\mathbf{BN}]$. Initially, two ion pairs with different relative cation−anion positions were optimized. The two minima correspond to $[\mathbf{Zr^{NC2}THF}][\mathbf{BN}]_{\mathbf{front}}$, where the anion is positioned close to the THF ligand, and $[\mathbf{Zr^{NC2}THF}][\mathbf{BN}]_{\mathbf{lateral}}$, where the anion is shifted toward the side of the $Zr-CH_2-N$ group as shown in Figure 5. In both cases the methyl group of the anion is oriented far away from the metal center.

In agreement with NOE results, the optimized structure of $[\mathbf{Zr^{NC2}THF}][\mathbf{BN}]_{\mathbf{front}}$ is more stable by 10.0 kJ mol^{-1}, despite the fact that the Zr−B distance is about 0.25 Å shorter in $[\mathbf{Zr^{NC2}THF}][\mathbf{BN}]_{\mathbf{lateral}}$ than in $[\mathbf{Zr^{NC2}THF}][\mathbf{BN}]_{\mathbf{front}}$. A reasonable explanation can be found by considering the dipole moments of the ion pairs. In fact, in low polar solvents, a higher stability is expected for species having a smaller charge separation. The computed dipole moments of $[\mathbf{Zr^{NC2}THF}][\mathbf{BN}]_{\mathbf{front}}$ and $[\mathbf{Zr^{NC2}THF}][\mathbf{BN}]_{\mathbf{lateral}}$ are 22.6 and 29.6 D, respectively. This suggests that the positive charge in the cation is partially shifted toward the nitrogen atom and the THF ligand.

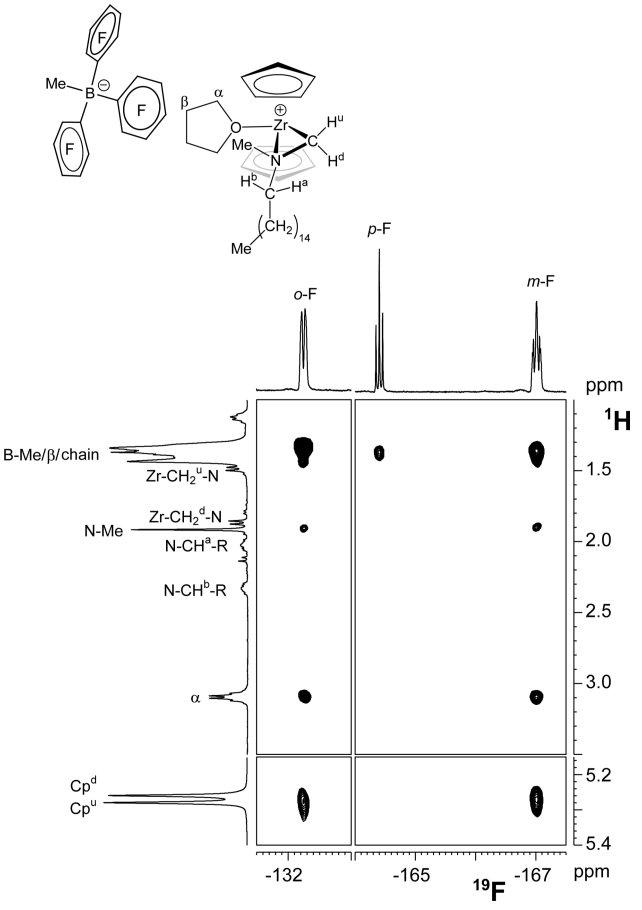

Figure 4. Four sections of the $^{19}F,^1H$ HOESY NMR spectrum of $[\mathbf{Zr^{NC16}THF}][\mathbf{BN}]$ (376.47 MHz, benzene-d_6, 297 K), showing the relevant interionic interactions. Note the absence of dipolar interactions between the anion and the $Zr-CH_2-N$ protons.

3. Self-Aggregation by PGSE NMR. Self-aggregation was investigated for all ion pairs shown in Scheme 2 by means of PGSE NMR measurements (Tables 1 and 2). This technique allows a fast and reliable estimation of the translational self-diffusion coefficient (D_t) from which the average hydrodynamic radius (r_H) of the diffusing species in solution is derived by means of the modified Stokes−Einstein equation:[36]

$$D_t = \frac{kT}{c\pi\eta r_H}$$

where k is the Boltzmann constant, T is the temperature, c is a numerical factor that depends on the ratio between r_H and the hydrodynamic volume of the solvent (r_{solv}), and η is the solution viscosity. From r_H, the average hydrodynamic volume (V_H) of the diffusing particle is obtained, assuming that the latter has a spherical shape. Finally, the ratio

(34) (a) Macchioni, A. *Eur. J. Inorg. Chem.* **2003**, 195. (b) Ciancaleoni, G.; Zuccaccia, C.; Zuccaccia, D.; Macchioni, A. In *Techniques in Inorganic Chemistry*; Fackler, J. P., Jr., Falvello, L., Eds.; CRC Press Taylor & Francis Group: Boca Raton, FL, 2010; pp 129−180. (c) Neuhaus, D.; Williamson, M. *The Nuclear Overhauser Effect in Structural and Conformational Analysis*; Wiley-VCH: New York, 2000. (c) Macura, S.; Ernst, R. R. *Mol. Phys.* **1980**, *41*, 95.

(35) Correa, A.; Cavallo, L. *J. Am. Chem. Soc.* **2006**, *128*, 10952.

(36) (a) Gierer, A.; Wirtz, K. Z. *Z. Naturforsch., A: Astrophys., Phys., Phys. Chem.* **1953**, *8*, 522. (b) Gierer, A.; Wirtz, K. Z. *Z. Naturforsch., A: Astrophys., Phys., Phys. Chem.* **1953**, *8*, 532. (c) Chen, H.-C.; Chen, S.-H. *J. Phys. Chem.* **1984**, *88*, 5118. (d) Zuccaccia, D.; Macchioni, A. *Organometallics* **2005**, *24*, 3476.

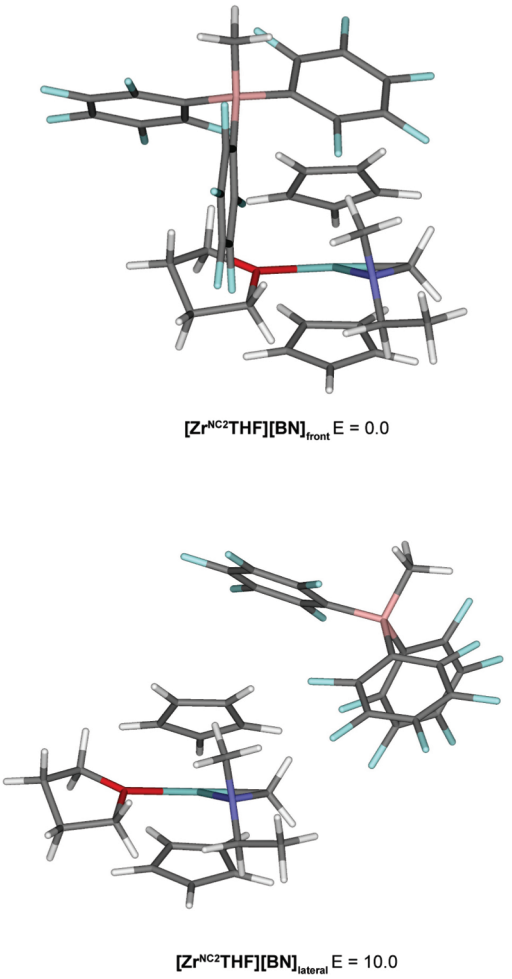

Figure 5. Optimized geometries and relative energies (in kJ mol^{-1}) for two different cation−anion orientations of [**Zr^{NC2}THF**][**BN**].

between V_H and the hydrodynamic volume of the elemental building block that form the supramolecular aggregate (V_H^0) affords the aggregation number N. Taking into account the low polarity of the solvents (benzene $\varepsilon_r = 2.28$, cyclohexane $\varepsilon_r = 2.04$), dissociation of ion pairs into free ions can be neglected.[37] Consequently, we can reasonably assume that the elemental aggregating unit is the whole ion pair for all the ISIPs and OSIPs. V_H^0 values for ISIPs containing the **BN** anion were obtained from the V_H values at different concentrations by extrapolation at infinite dilution.[38,39] V_H^0 values for ISIPs containing the **BT** anion were estimated by subtracting the hydrodynamic volume of the **BN** anion from the corresponding ISIP and then adding the hydrodynamic volume of the **BT** anion (605 Å^3).[40] The hydrodynamic volume of the **BN** anion was estimated by considering that the ratio between the van der Waals volumes of

(37) For example, it is known that, at concentrations below 10^{-5} M, the fraction of ammonium salt existing as free ions amounts to one part per million or less: Copenhafer, D. T.; Kraus, C. A. *J. Am. Chem. Soc.* **1951**, *73*, 4557.

(38) Ciancaleoni, G.; Zuccaccia, C.; Zuccaccia, D.; Macchioni, A. *Organometallics* **2007**, *26*, 3624and references therein.

(39) Macchioni, A.; Ciancaleoni, G.; Zuccaccia, C.; Zuccaccia, D. *Chem. Soc. Rev.* **2008**, *37*, 479.

(40) Rocchigiani, L.; Bellachioma, G.; Ciancaleoni, G.; Crocchianti, S.; Laganà, A.; Zuccaccia, C.; Zuccaccia, D.; Macchioni, A. *ChemPhysChem* **2010**, *11*, 3243.

Table 1. Diffusion Coefficients (D_t, 10^{-10} m^2 s^{-1}),[a] Hydrodynamic Radii (r_H, Å), Hydrodynamic Volumes (V_H, Å^3), and Aggregation Numbers (N) for ISIPs and OSIPs in Benzene-d_6 (r_{solv} = 2.6 Å, ε_r = 2.28) at 297 K and Different Concentrations (C, 10^{-3} M)

compd (V_H^0)	C	D_t	r_H	V_H	N
Zr^{NC2}BN (829)	0.86	6.29	5.82	825	1.0
	2.67	6.21	5.88	851	1.0
	6.37	6.17	5.91	864	1.0
	13.56	5.82	6.20	998	1.2
Zr^{NC16}BN (1284)	0.6	5.26	6.75	1 290	1.0
	2.7	5.09	6.95	1 410	1.1
	7.4	5.11	6.92	1 390	1.1
	13.4	4.89	7.18	1 550	1.2
Zr^{NC18}BN (2088)	0.56	4.40	7.94	2 100	1.0
	1.11	4.37	7.94	2 100	1.0
	2.63	4.34	7.98	2 130	1.0
	25.0	4.11	8.39	2 470	1.2
Zr^{NPh}BN (870)	3.8	6.13	5.94	877	1.0
	35.1	5.21	6.81	1 320	1.5
Zr^{NPh}BT (985)	0.1	5.80	6.23	1 010	1.0
	0.31	5.61	6.40	1 100	1.1
	0.65	5.35	6.66	1 240	1.3
	1.1	5.18	6.85	1 350	1.4
	1.8	4.84	7.26	1 600	1.6
	3.5[b]	4.34	8.0	2 140	2.2
Zr^{NC18}BT (2203)	0.14	4.36	8.0	2 170	1.0
	0.86	3.81	9.0	3 010	1.4
	2.8	3.17	10.7	5 060	2.3
	4.4	2.93	11.5	6 350	2.9
	9.9	2.55	13.1	9 470	4.3
	19.8	2.17	15.1	15 050	6.8
	32.4	1.87	17.6	23 060	10.5
[**Zr^{NC2}THF**][**BN**] (899)	0.09	5.98	6.06	932	1.0
	0.23	5.85	6.18	988	1.1
	0.42	5.23	6.78	1 300	1.5
	0.98[b]	4.86	7.23	1 580	1.8
[**Zr^{NC16}THF**][**BN**] (1354)	0.12	4.77	7.34	1 660	1.2
	0.32	4.34	7.81	1 990	1.5
	0.59	4.30	8.04	2 180	1.6
	1.6	3.85	8.90	2 950	2.2
	1.8	3.83	8.95	3 000	2.2
	3.88	3.44	9.89	4 050	3.0
	6.2	3.15	10.7	5 190	3.8
	8.45[b]	2.89	11.6	6 570	4.9
[**Zr^{NC18}THF**][**BN**] (2158)	0.11	4.17	8.28	2 380	1.1
	0.49	3.84	8.91	2 960	1.4
	1.09	3.50	9.73	3 860	1.8
	3.02	3.10	10.9	5 420	2.5
	6.63	2.74	12.3	7 795	3.6
	7.07	2.68	12.5	8 160	3.8
	11.7	2.37	14.0	11 600	5.4
[**Zr^{NPh}THF**][**BN**] (940)	0.67	5.01	7.05	1 470	1.6
[**Zr^{NPh}THF**][**BT**] (1055)	0.56	4.79	7.2	1 540	1.5
	1.3	4.26	8.1	2 240	2.1
[**Zr^{NC18}THF**][**BT**] (2273)	0.26	3.76	9.1	3 130	1.4
	0.67	3.33	10.2	4 390	1.9
	1.55	3.20	10.5	4 920	2.2
	6.74	2.65	12.6	8 390	3.7
	13.9	2.18	15.2	14 760	6.5

[a] The reported values have been corrected for changes in solution viscosity due to the increased ion pair concentration using the residual solvent resonance as an internal standard.[36d,50] [b] Saturated solution.

Table 2. Diffusion Coefficients (D_t, 10^{-10} m^2 s^{-1}), Hydrodynamic Radii (r_H, Å), Hydrodynamic Volumes (V_H, Å^3), and Aggregation Numbers (N) for ISIPs and OSIPs in Cyclohexane-d_{12} (r_{solv} = 2.8 Å, ε_r = 2.04)[a] at 297 K and Different Concentrations (C, 10^{-3} M)

compd (V_H^0)	C	D_t	r_H	V_H	N
Zr^{NC16}BN (1490)	0.083	3.36	7.08	1 490	1.0
	0.26	3.37	7.08	1 490	1.0
	0.95	3.31	7.18	1 550	1.0
	3.25	3.22	7.35	1 660	1.1
	5.42	3.00	7.81	1 990	1.3
	8.3	2.77	8.38	2 460	1.7
Zr^{NC18}BN (2620)	0.076	2.67	8.66	2 720	1.0
	0.5	2.71	8.55	2 620	1.0
	1.45	2.69	8.61	2 670	1.0
	3.36	2.62	8.82	2 870	1.1
	8.2	2.35	9.72	3 840	1.5
	15.8	2.06	11.0	5 560	2.1
[Zr^{NC16}THF][BN] (2620)	0.036[b]	2.62	8.82	2 870	1.8
[Zr^{NC18}THF][BN] (2690)	0.05	2.01	11.2	5 910	2.2
	0.90	1.44	15.4	15 400	5.7
	1.60	1.22	18.2	25 200	9.4
	2.47	1.11	19.8	32 700	12.2
	4.75	0.97	22.8	49 800	18.5
	11.8	0.78	28.3	94 700	35.2
	19.0	0.68	32.3	141 000	52.4
	23.2	0.65	33.8	162 000	60.2
[Zr^{NC18}THF][BT] (2760)	0.26	1.76	12.7	8 640	3.1
	0.8	1.32	16.8	19 890	7.2
	4.27	1.02	22.0	44 100	16.0
	7.9	0.78	28.0	91 610	33.2
	10.33	0.72	30.7	121 020	43.9
	17.26	0.64	34.4	171 170	62.0
	25.23	0.54	40.9	287 000	104.0

[a] Benzene (80 mM) was added as PGSE internal standard. [b] Saturated solution.

BN and **BT** anions (V_{vdW}(**BT**)/V_{vdW}(**BN**) = 1.236) is equal to the ratio between their corresponding hydrodynamic volumes. Finally, V_H^0 values for all the OSIPs were computed by adding the hydrodynamic volume of THF (70 Å^3) to the V_H^0 values of the corresponding ISIPs.

3.1. Effect of Anion and R Substituents on Nitrogen. 3.1.1. Ion Pairs Containing the BN Anion. The trends of N vs C (concentration) in benzene-d_6 for ion pairs bearing the **BN** anion (Figure 6) clearly show different behaviors of ISIPs and OSIPs, as previously found.[4d,9,10]

For ISIPs, N deviates very little from 1, indicating a negligible tendency to self-aggregate. In solution these species are mainly present as ion pairs and a small amount of higher aggregates start to be present only at fairly high concentration (N = 1.5 at 35.1 mM for **Zr^{NPh}BN**). In contrast, N values of OSIPs rapidly increase when the concentration is increased, approaching 2 already at concentrations around 1 mM. This indicates an increased tendency to form higher order ionic aggregates. Nevertheless, N values for OSIPs approaches 1 at high dilution (ca. 10^{-5} M), indicating the prevalence of ion pairs at very low concentration. Concerning the effect of the R substituents on the nitrogen atom, the experimental data show that increasing the length of the alkyl chain or substituting an alkyl with an aryl group has no effect on self-aggregation. On the other hand, the nature of the alkyl chain dramatically changes the solubility of OSIPs: for example, concentration of a saturated solution of **[Zr^{NC2}THF][BN]** is around 1 mM and that of **[Zr^{NC18}THF][BN]**

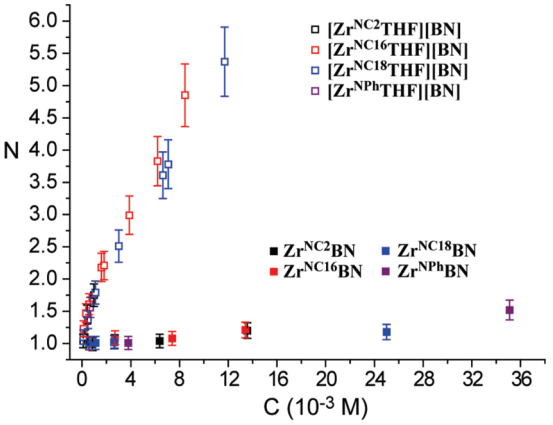

Figure 6. Trends of the aggregation number (N) as a function of the analytical concentration (C) for **BN**-containing ISIPs (solid symbols) and OSIPs (open symbols) in benzene-d_6 at 297 K.

is higher than 11.7 mM in benzene-d_6. A coherent picture is derived from NOE and PGSE measurements in benzene-d_6. NOE experiments indicate that the position and distance of the counterion from the metal center is little affected by the nature of the R substituent; consequently the latter has no appreciable effect on the overall dipole moment and self-aggregation tendencies of ion pairs observed by means of diffusion experiments.

3.1.2. Ion Pairs Containing the BT Anion. The data of N at different concentrations in benzene-d_6 for ion pairs bearing the **BT** anion are reported in Table 1. The variation of the aggregation number of OSIPs (**[Zr^{NPh}THF][BT]** and **[Zr^{NC18}THF][BT]**) is very similar to that observed for all the other OSIPs containing the **BN** anion. It thus appears that the nature of the anion has only a marginal effect on the self-aggregation of OSIPs. This is in agreement with the NOE data discussed above, where it was noted that the interionic structures of OSIPs are substantially the same for both the **BN** and **BT** anions. As discussed above, the **BN** anion possesses an increased rotational freedom when it is forced into the second coordination sphere. Consequently, only small differences are expected between the dipole moment of corresponding OSIPs having either the **BT** or the **BN** anion (for example, the computed dipole moments of **[Zr^{NC2}THF][BN]** and **[Zr^{NC2}THF][BT]** are 22.3 and 25.9 D, respectively) and a similar tendency to form larger ionic aggregates is observed.

The ion pairs **Zr^{NPh}BT** and **Zr^{NC18}BT** appear to behave differently from either ISIP or OSIP. N values of **Zr^{NPh}BT** substantially deviate from 1 when the concentration is increased, even if the aggregation is slightly reduced with respect to those of **[Zr^{NPh}THF][BN]** and **[Zr^{NPh}THF][BT]**. For example, the N value of **Zr^{NPh}BT** is 2.2 at 3.5 mM, while that of **[Zr^{NPh}THF][BT]** is 2.1 at 1.3 mM (Table 1). A similar trend is observed for **Zr^{NC18}BT**: its tendency to self-aggregate is much higher than that of **Zr^{NC18}BN** and close to those of **[Zr^{NC18}THF][BN]** and **[Zr^{NC18}THF][BT]**. This can be explained by considering that the dipole moments of **BT**-containing ISIPs are much higher than those of the corresponding **BN**-containing ISIPs and are similar to the dipole moments of OSIPs. DFT calculations carried out on ion pairs bearing the **NC2** moiety are consistent with the previous hypothesis. In fact, two minima were found for **Zr^{NC2}BT**. The ion pair in which the anion interacts with the metal center through one fluorine atom in a meta

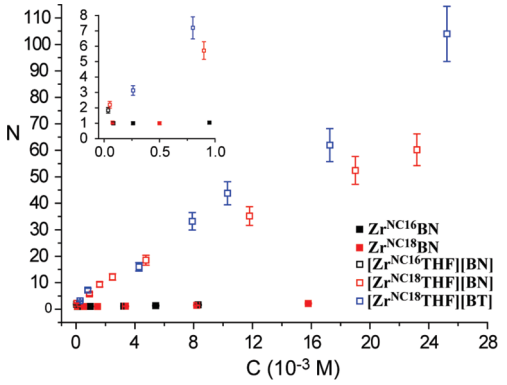

Figure 7. Trends of the aggregation number (N) as a function of the analytical concentration (C) for ISIPs (filled symbols) and OSIPs (open symbols) in cyclohexane-d_{12} at 297 K.

position (**Zr^{NC2}BT^{m}**) is about 8.4 kJ mol^{-1} more stable than that where the anion approaches the cation with one fluorine atom in a para position (**Zr^{NC2}BT^{p}**). In agreement with diffusion data, the computed dipole moment of **Zr^{NC2}BT^{m}** is 24.4 D. This value is very similar to that of [**Zr^{NC2}THF**]-[**BN**]$_{front}$ (22.6 D) and much higher than that of **Zr^{NC2}BN** (17.1 D). On a closer look, it also appears that the aggregation tendency of **Zr^{NC18}BT** is slightly larger than that of **Zr^{NPh}BT**, suggesting an higher degree of charge separation in **Zr^{NC18}BT**. This can just be due to the higher steric requirements of the two C18 tails, but an electronic contribution is also possible. It may be hypothesized, for example, that one of the two C18 tails folds back toward the metal center and establishes a weak agostic interaction between one of the CH_2 moieties of the chain and the zirconium. This would result in the displacement of the anion into the second coordination sphere with a consequent increase of charge separation within the ion pair. A weak support for this hypothesis comes from NMR spectroscopy. In fact, the two N−CH_2−R moieties of the two C18 tails appear as separate signals in the ^{1}H NMR spectrum (δ_H 2.65 and 2.50 ppm), suggesting that the plane defined by the azazirconacyclopropane ring no longer represents a plane of symmetry for **Zr^{NC18}BT.**

3.2. Effect of Solvent Polarity. The enhanced solubility of zirconaaziridinium ion pairs bearing long alkyl chains prompted us to explore their self-aggregation behavior in a solvent having a relative permittivity smaller than that of benzene. We chose cyclohexane, because its features (aliphatic character and dielectric constant, $\varepsilon_r = 2.04$) are very similar to those of commercial ISOPAR[41] commonly used in industrial plants for olefin polymerizations. Diffusional and hydrodynamic data in cyclohexane-d_{12} for ion pairs containing C16 and C18 tails are reported in Table 2 and Figure 7.

As can be seen from Table 2, the self-aggregation tendency of ISIPs is only slightly increased on passing from benzene-d_6 to cyclohexane-d_{12}. For example, for a 7.4 mM solution of **Zr^{NC16}BN** in benzene-d_6 N is equal to 1.1, while, at almost the same concentration (5.4 mM) in cyclohexane-d_{12}, N amounts to 1.3. In sharp contrast, the self-aggregation of OSIPs is remarkably higher in cyclohexane-d_{12} than in benzene-d_6. While for a 1.1 mM solution of [**Zr^{NC18}THF**][**BN**] in benzene-d_6 N is equal to 1.8, at almost the same concentration

(41) ISOPAR is a trademark of Exxon Mobil Corporation. For more information see: http://www.exxonmobilchemical.com

Table 3. Equations To Calculate the Weight Fraction of the Monomer (A) and Aggregation Number (N) for EK, AK, and IK Models[a]

model	α	N
EK	$\alpha^2L^2 - \alpha(2L+1) + 1 = 0$	$(1-\alpha L)$
AK	$\alpha - e^{-\alpha L} = 0$	$L/[(1/\alpha) - 1]$
IK	$\alpha(L+1) - 1 = 0$	$L/[\ln(L+1)]$

[a] L is defined as $L = KC$, where C is the analytical molar concentration of the monomer.

(1.6 mM) in cyclohexane-d_{12}, N amounts to 9.4. Aggregates containing an average of 104 ion pairs are present for [**Zr^{NC18}THF**][**BT**] in cyclohexane-d_{12} at the highest concentration, while, at submillimolar concentration (0.05 mM), N is still 2.2 for [**Zr^{NC18}THF**][**BN**]. Although [**Zr^{NC16}THF**][**BN**] was not soluble enough in cyclohexane-d_{12} to allow a complete PGSE study as a function of the concentration, the N value measured for its saturated solution (0.04 mM) amounts to 1.8 and fits rather well in the N versus C trends of [**Zr^{NC18}THF**][**BN**] and [**Zr^{NC18}THF**][**BT**] (Figure 7, inset). We conclude that also in cyclohexane-d_{12} the chain length has a negligible effect on the self-aggregation tendency of OSIPs.

3.3. Thermodynamic Parameters of the Self-Aggregation Process. From the discussion above, it is clear that, as the total concentration is increased, N steadily increases to values much larger than 2 for OSIPs. Thus, the aggregation process proceeds beyond the formation of ion quadruples. The tendency of ISIPs and OSIPs to self-aggregate has been quantified using models of indefinite self-association.[42] Ion pairs were considered as the elemental aggregating unit (A) that may self-aggregate forming ion quadruples (A_2), ion hextuples (A_3), etc... as represented by the following equations:

$$A + A = A_2 \quad K_2 = \frac{[A_2]}{[A]^2}$$

$$A_2 + A = A_3 \quad K_3 = \frac{[A_3]}{K_2[A]^3}$$

...

$$A_{i-1} + A = A_i \quad K_i = \frac{[A_i]}{[A]^i \prod_{i=2}^{i-1} K_i}$$

Three different indefinite self-association models were taken into account.[43] In the EK (equal K) model each step is characterized by the same equilibrium constant ($K_2 = K_3 = ... = K_i = K_E$), while, in the AK (attenuated K) model, the equilibrium constants decrease following the relation $2K_2 = 3K_3 =$

(42) Martin, R. B. *Chem. Rev.* **1996**, *96*, 3043and references therein.

(43) For a review concerning the application of the indefinite self-association models in supramolecular polymerizations see: (a) De Greef, T. M. A.; Smulders, M. M. J.; Wolffs, M.; Schenning, A. P. H. J.; Sijbesma, R. P.; Meijer, E. W. *Chem. Rev.* **2009**, *109*, 5687and references therein. For other examples see: (b) Rymden, R.; Stilbs, P. *Biophys. Chem.* **1985**, *21*, 145. (c) Stokkeland, I.; Stilbs, P. *Biophys. Chem.* **1985**, *22*, 65. (d) Regan, D. G.; Chapman, B. E.; Kuchel, P. W. *Magn. Reson. Chem.* **2002**, *40*, S115. (e) Zhao, D.; Moore, J. S. *Chem. Commun.* **2003**, 807. (f) Chen, Z.; Stepanenko, V.; Dehm, V.; Prins, P.; Siebbeles, L. D. A.; Seibt, J.; Marquetand, P.; Engel, V.; Würthner, F. *Chem. Eur. J.* **2007**, *13*, 436.

Table 4. Limiting Equilibrium Constants and Corresponding Standard Gibbs Free Energies at 297 K for the Indefinite Self-Aggregation (EK, AK, and IK Models) of ISIPs and OSIPs Bearing C18 Tails in Benzene-d_6 and Cyclohexane-d_{12}

	model					
	EK		AK		IK	
compd	K_E[a]	$-\Delta G^0$(EK)[b]	K_A[a]	$-\Delta G^0$(AK)[b]	K_I[a]	$-\Delta G^0$(IK)[b]
			Benzene-d_6			
[**Zr^{NC18}**][**BN**]	8.49 ± 0.55[c] (0.005 623)[d]	5.3 ± 0.2	19.09 ± 4.19 (0.006 286)	7.3 ± 0.5	15.2 ± 0.96 (0.005 955)	6.7 ± 0.2
[**Zr^{NC18}**][**BT**]	2 250 ± 783 (2.175)	19.1 ± 0.9	73 613 ± 62 205 (5.65)	27.8 ± 2.1	1 145 ± 61 (0.514 7)	17.5 ± 0.2
[**Zr^{NC18}THF**][**BN**]	1 628 ± 302 (0.639)	18.3 ± 0.5	17 124 ± 12 500 (1.77)	24.2 ± 1.8	1 248 ± 72 (0.285 6)	17.7 ± 0.2
[**Zr^{NC18}THF**][**BT**]	2 156 ± 743 (0.865)	19.0 ± 0.9	32 084 ± 27 375 (2.27)	25.7 ± 2.1	1 392 ± 268 (0.708)	17.9 ± 0.5
			Cyclohexane-d_{12}			
[**Zr^{NC18}**][**BN**]	114 ± 53 (0.327)	12 ± 1	334 ± 182 (0.43)	14.4 ± 1.4	160 ± 42 (0.23)	12.6 ± 0.7
[**Zr^{NC18}THF**][**BN**]	122 991 ± 34 358 (13.82)	29.0 ± 0.7			15 589 ± 595 (3.18)	23.9 ± 0.1
[**Zr^{NC18}THF**][**BT**]	250 751 ± 133 438 (34.22)	30.8 ± 1.3			24 286 ± 2 941 (13.44)	25.0 ± 0.3

[a] In M^{-1}. [b] In kJ mol^{-1}. [c] Error intervals are given at 95% confidence. [d] The numbers in parentheses represent the Euclidean norm of the residuals with respect to the experimental N values.

$4K_4 = ... = iK_i = K_A$. Finally, in the IK model, successive equilibrium constants mildly increase according to the relation $2K_2 = 3K_3/2 = 4K_4/3 = ... = iK_i/(i-1) = K_I$. From these relationships and the equations above, the weight fraction of the monomer (α) and the aggregation number (N) can be analytically formulated. Related expressions are given in Table 3. In each formulation, α is given as a function of the analytical concentration C and the corresponding equilibrium constant K via the variable $L = KC$.

All three models of indefinite self-aggregation described above have been used for the single-parameter (K_E, K_A, or K_I) nonlinear least-squares fit of N data as a function of the analytical concentration using a Fortran code reported in a recent paper.[40] Initially, ion pairs bearing C18 tails were taken into account, because, thanks to the high solubility of these complexes, the experimental data extend over a relatively large concentration range in both benzene and cyclohexane. The results of the fitting procedure are reported in Table 4. As an example, Figure 8 shows the best-fit curves obtained for **Zr^{NC18}BN** and [**Zr^{NC18}THF**][**BN**] in cyclohexane-d_{12}.

We found that the IK model always gives the best fit to the experimental data points: only in the case of **Zr^{NC18}BN** in benzene-d_6 is the best fit obtained with the EK model. The fact that better fits are obtained with the IK model suggests a sort of mild cooperativity, where the addition of an ion pair to a given aggregate is somewhat progressively more exergonic as the average size of the aggregate increases. From the computed limiting equilibrium constants (K_I), the corresponding standard Gibbs free energies of self-association (ΔG^0) at 297 K are calculated and shown in Table 4. The quantitative analysis is in good agreement with the qualitative discussion reported above. In benzene-d_6, ΔG^0 of **Zr^{NC18}BN** amounts to −6.7 kJ mol^{-1}. ΔG^0 decreases to approximately −17.7 kJ mol^{-1} for **Zr^{NC18}BT**, [**Zr^{NC18}THF**][**BN**], and [**Zr^{NC18}THF**][**BT**] as a consequence of an increased charge separation. Changing the solvent from benzene-d_6 to cyclohexane-d_{12} resulted in a remarkable increase of the aggregation tendency.[43b,44] For instance, the ΔG^0 of [**Zr^{NC18}THF**][**BT**] is −25 kJ mol^{-1} in cyclohexane-d_{12}.

From the values of α and K_I, the distribution of i-mers in terms of their weight fractions (α_i) can be computed at a given analytical concentration using the equation

$$\alpha_i = \alpha^i L^{i-1}$$

Figure 9 shows the distributions of i-mers at four different analytical concentrations ranging from 10^{-6} M to 10^{-3} M for [**Zr^{NC18}THF**][**BT**] in benzene-d_6 (top) and cyclohexane-d_{12} (bottom). The distributions are plotted to an oligomerization order (i) up to 10, even though the model accounts for an indefinite self-association.

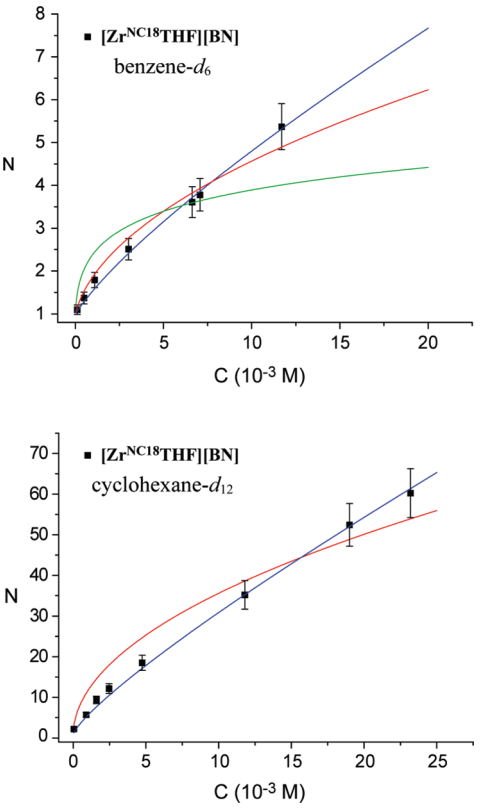

Figure 8. Trends of the aggregation number (N) as a function of the analytical concentration (C) for [**Zr^{NC18}THF**][**BN**] in benzene-d_6 (top) and cyclohexane-d_{12} (bottom) at 297 K. Solid lines represent best fits to the data using the EK (red), AK (green), and IK (blue) indefinite self-aggregation models.

(44) (a) Haino, T.; Tanaka, M.; Fukazawa, Y. *Chem. Commun.* **2008**, 468. (b) Kraft, A.; Osterod, F.; Frhölich, R. *J. Org. Chem.* **1999**, *64*, 6425.

In benzene-d_6 the total amount of aggregates larger than simple ion pairs becomes appreciable only at concentrations larger than 10^{-4} M. In contrast, the relative concentrations of quadruples and larger aggregates become substantial (around 20%) already at 10^{-5} M in cyclohexane-d_{12}. At the analytical concentration of 10^{-3} M, only 40% and 4% of [**Zr^{NC18}THF**][**BT**] is present as ion pairs, in benzene-d_6 and cyclohexane-d_{12}, respectively.

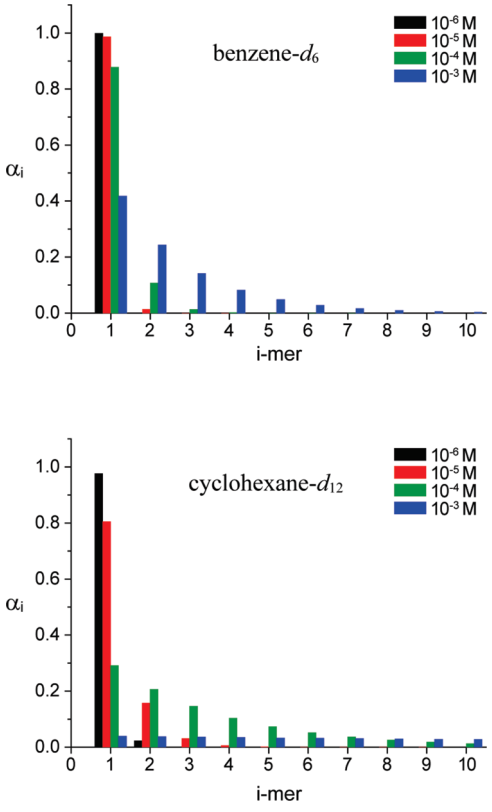

Figure 9. Estimated weight fractions (α_i) of *i*-mers (1-mer = ion pair, 2-mer = ion quadruple, 3-mer = ion hextuples, ...) at *C* equal to 10^{-6} M (black), 10^{-5} M (red), 10^{-4} M (green), and 10^{-3} M (blue) for [**Zr^{NC18}THF**][**BT**] in benzene-d_6 (top) and cyclohexane-d_{12} (bottom).

To gain further insight into the thermodynamics of the aggregation process, temperature-dependent NMR diffusion measurements were performed for [**Zr^{NC18}THF**][**BN**] in cyclohexane-d_{12}. Table 5 summarizes D_t, r_H, V_H, N, K_I, and ΔG^0 values at 297, 300.2, 313.6, and 328.3 K, as well as an estimation of the standard enthalpy (ΔH^0) and standard entropy (ΔS^0) obtained from the van't Hoff plot (Figure 10). Increasing the temperature results in a drastic reduction of the aggregation tendency. At 11.8 mM, *N* for [**Zr^{NC18}THF**][**BN**] decreases from 35.2 to 11.9 on passing from 297 to 328.3 K. Quantitative analysis using the van't Hoff approximation shows that the limiting aggregation step is characterized by a ΔH^0 value of about -33 ± 10 kJ mol^{-1}.

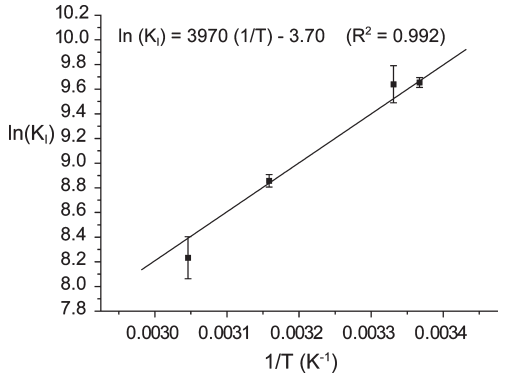

Figure 10. van't Hoff plot for the equilibrium $A_{i-1} + A = A_i$ ($i \rightarrow \infty$) according to the IK model.

Table 5. Diffusion Coefficients (D_t, 10^{-10} m^2 s^{-1}), Hydrodynamic Radii (r_H, Å), Hydrodynamic Volumes (V_H, Å^3), Aggregation Numbers (*N*), and K_I (M^{-1}), ΔG^0 (kJ mol^{-1}), ΔH^0 (kJ mol^{-1}), and ΔS^0 (J mol^{-1} K^{-1}) Values[a] for [Zr^{NC18}THF][BN] in Cyclohexane-d_{12} (ε_r = 2.04)[b] at Different Temperatures (*T*, K) and Concentrations (*C*, 10^{-3} M)

T	*C*	D_t	r_H	V_H	*N*	K_I	$-\Delta G^0$	$-\Delta H^0$	$-\Delta S^0$
297.0	0.05	2.01	11.2	5 910	2.2	15 589 ± 595	23.9 ± 0.1	33 ± 10	31 ± 33
	0.90	1.44	15.4	15 400	5.7				
	1.60	1.22	18.2	25 200	9.4				
	2.47	1.11	19.8	32 700	12.2				
	4.75	0.97	22.8	49 800	18.5				
	11.8	0.78	28.3	94 700	35.2				
	19.0	0.68	32.3	141 000	52.4				
	23.2	0.65	33.8	162 000	60.2				
300.2	0.9	1.44	15.5	15 600	5.8	15 368 ± 2 274	23.9 ± 0.4		
	1.6	1.22	18.2	25 200	9.4				
	2.47	1.10	20.2	34 400	12.8				
	4.75	0.98	22.5	47 600	17.7				
	11.8	0.79	27.8	89 900	33.4				
313.6	0.9	1.84	12.2	7 510	2.8	7 024 ± 352	21.9 ± 0.1		
	1.6	1.61	13.8	10 900	4.1				
	2.47	1.42	15.7	16 000	6.0				
	4.75	1.21	18.2	25 200	9.4				
	11.8	0.96	23.0	50 800	18.8				
328.3	0.9	2.19	10.4	4 680	1.7	3 764 ± 639	20.4 ± 0.4		
	1.6	2.01	11.2	5 850	2.2				
	2.47	1.70	13.1	9 500	3.5				
	4.75	1.38	16.1	17 300	6.4				
	11.8	1.13	19.7	31 900	11.9				

[a] Error intervals are given at 95% confidence. [b] Benzene (80 mM) was added as PGSE internal standard.

At the 95% confidence level, the error associated with ΔS^0 is rather large, but the average negative value of -31 J mol^{-1} K^{-1} strongly suggests an enthalpy-driven self-aggregation process. Most likely, electrostatic interactions give a larger contribution to the overall interaction enthalpy, but, considering the large differences observed on passing from benzene-d_6 to cyclohexane-d_{12}, other weak forces, including van der Waals and solvophobic interactions, may also be important.

Conclusions

Up to now, the interionic structure and level of aggregation of metallocenium ion pairs have been studied mostly by varying the nature of the anion and/or the metallocene skeleton, whereas only Me or CH_2TMS groups were used as models for the polymer chain.[4f−h,7,9,10] In this work, we have investigated zirconaaziridinium ion pairs bearing long alkyl chains of different lengths that would better mimic the growing polymer chain. The azazirconacyclopropane structure imparts high stability to the cation, allowing us to compare the behavior of ion pairs containing either the **BN** and **BT** counterions under strictly similar conditions. The results indicate that for **BN**-containing ISIPs and for all OSIPs increasing the length of the alkyl chain or substituting an alkyl with an aryl group has no effect on the self-aggregation tendency, since the anion position and, consequently, the dipole moment of the ion pair are almost unaffected by the length of the chain. Instead, it seems that there is a small increment of the self-aggregation tendency on passing from $\mathbf{Zr^{NPh}BT}$ to $\mathbf{Zr^{NC18}BT}$, suggesting that the steric/electronic properties of the different R substituents on the nitrogen atom may weakly influence the strength of the cation−anion interaction in the case of ISIP containing the weakly coordinating **BT** anion. The self-aggregation is strongly affected by the nature of the anion only in the case of ISIPs. The bulkier and less coordinating **BT** anion affords ion pairs displaying aggregation tendencies much higher than those of **BN**-containing ISIPs and similar to those of OSIPs. The effect of the solvent is dramatic: the level of aggregation increases about 10 times on passing from benzene (ε_r = 2.28) to cyclohexane (ε_r = 2.02). As a consequence, the percentage of ion quadruples or higher ionic aggregates in cyclohexane is not negligible even at very low concentration. For instance, the percentage of ion quadruples and higher aggregates is about 20% for a 10^{-5} M solution of OSIPs in cyclohexane. Finally, the self-aggregation is strongly depressed by increasing the temperature ($\Delta H^0 = -33 \pm 10$ kJ mol^{-1} and $\Delta S^0 = -31 \pm 33$ J mol^{-1} K^{-1} for $[\mathbf{Zr^{NC18}THF}][\mathbf{BN}]$ in cyclohexane). This dependence on temperature suggests that the presence of ionic aggregates larger than ion pairs may be negligible in high-temperature solution polymerization process usually used in industrial plants.

Experimental Section

General Procedures. All manipulations of air-sensitive materials were performed in flamed Schlenk glassware on a Schlenk line, interfaced to a high-vacuum pump (10^{-5} mmHg), or in a nitrogen-filled glovebox with a high-capacity recirculator (< 1 ppm of O_2 and H_2O). All solvents were preventively distilled after 12 h of reflux over Na and freeze−pump−thaw degassed over Na/K alloy. Deuterated solvents were freeze−pump−thaw degassed (benzene-d_6 and cyclohexane-d_{12} over Na/K alloy, chlorobenzene-d_5 over CaH_2) and vacuum-transferred to a storage Schlenk with a PTFE valve. Cp_2ZrCl_2 (≥98%) and LiMe (1.6 M solution in Et_2O) were purchased from Aldrich and used without further purifications. The liquid amines (Aldrich) NMe_2Et, $NMe_2C_{16}H_{33}$, and $NMe_2C_6H_5$ were freeze−pump−thaw degassed after 12 h of stirring over CaH_2 and vacuum-transferred to a storage Schlenk. The solid amine $NMe(C_{18}H_{37})_2$ (≥99%, Aldrich) was used without further purification. $B(C_6F_5)_3$, $CPh_3^+B(C_6F_5)_4^-$, and $HNMe_2C_6H_5^+B(C_6F_5)_4^-$ were obtained as a gift from Dow Chemical. $B(C_6F_5)_3$ was purified by vacuum sublimation (60 °C, 5×10^{-5} mmHg), while the other activators were used as received. Cp_2ZrMe_2 ($\mathbf{Zr^{Me_2}}$)[45] and $[Cp_2ZrMe^+\cdots MeB(C_6F_5)_3^-]$ ($\mathbf{Zr^{Me}BN}$)[17a] were prepared according to the literature.

One- and two-dimensional ^{1}H, ^{13}C, and ^{19}F NMR spectra were measured on a Bruker DRX 400 spectrometer. Referencing is relative to external TMS (^{1}H and ^{13}C) and CCl_3F (^{19}F). ^{1}H NOESY[46] NMR experiments were acquired by the standard three-pulse sequence or by the PFG version.[47] Two-dimensional ^{19}F,^{1}H HOESY experiments were acquired using the standard four-pulse sequence or its modified version.[48] The number of transients and data points were chosen according to the sample concentration and desired final digital resolution. Qualitative or semiquantitative two-dimensional Overhauser spectra were recorded using a 1 s relaxation delay and 800 ms mixing time. NMR samples for standard NMR characterization were prepared inside the glovebox by dissolving the suitable amount of compound in approximately 0.7 mL of the suitable deuterated solvent.

Synthesis and Characterization. $[Cp_2Zr(\eta^2\text{-}CH_2NMeEt)^+\cdots MeB(C_6F_5)_3^-]$ ($\mathbf{Zr^{NC2}BN}$). In the glovebox, $\mathbf{Zr^{Me}BN}$ (25 mg, 32.6 mmol) was loaded into a J. Young NMR tube and dissolved in approximately 0.7 mL of benzene-d_6. A 1.5 equiv amount of NMe_2Et (5.3 μL) was added by a micrometric syringe, and the mixture was strongly shaken. In a few minutes, a dense oily phase settled to the bottom of the tube and gas evolution was observed. The supernatant solution was removed, and the residue was rinsed with benzene (3 × 1 mL) to remove the small excess of the amine. After 12 h, the J. Young NMR tube was interfaced to the high-vacuum line and the solvent removed in vacuo. Finally, the residue was rinsed with pentane (3 × 1 mL) and dried under high vacuum. The reaction product was an oil. A 2.7 mM solution of $\mathbf{Zr^{NC2}BN}$ in benzene-d_6 showed no sign of decomposition after 7 days.

^{1}H NMR (400.13 MHz, benzene-d_6, 297 K, J in Hz): δ 5.28 (s, Cp^u), 5.25 (s, Cp^d), 2.40 (m, $NCH_2{}^b$), 1.93 (m, $NCH_2{}^a$), 1.87 (s, NMe), 1.61 (d, $^2J_{H_u-H_d} = 8.3$, $ZrCH_2{}^d$), 1.34 (d, $^2J_{H_u-H_d} = 8.3$, $ZrCH_2{}^u$), 0.57 (br t, $^3J_{H_\omega-NCH_2} = 7.0$, ωMe), 0.11 (s, BMe). $^{13}C\{^1H\}$ NMR (100.55 MHz, benzene-d_6, 297 K): δ 110.3 (Cp^u), 110.2 (Cp^d), 64.8 (NCH_2), 54.6 ($ZrCH_2$), 48.0 (NMe), 9.1 (ωMe), −6.3 (BMe). ^{19}F NMR (376.65 MHz, benzene-d_6, 297 K, J in Hz): δ −132.8 (brd $^3J_{oF-mF} = 21.8$, *o-F*), −161.6 (t $^3J_{pF-mF} = 20.7$, *p-F*), −165.8 (m, *m-F*).

$[Cp_2Zr(\eta^2\text{-}CH_2NMe(C_{16}H_{33}))^+\cdots MeB(C_6F_5)_3^-]$ ($\mathbf{Zr^{NC16}BN}$). In the glovebox, $\mathbf{Zr^{Me}BN}$ (100 mg, 130.5 mmol) was loaded into a screw-top vial and 10 mL of benzene was added. The solution was lightly shaken, and 1.5 equiv of $NMe_2(C_{16}H_{33})$ (60 μL) was added with a micrometric syringe. After an intense shake, a dense oily phase was allowed to settle to the bottom of the vial. The supernatant solution was removed, and the residue was rinsed with benzene (3 × 2 mL). After 1 day, the oil was transferred to a flip frit apparatus interfaced to the high-vacuum line, washed with pentane, and finally dried. The reaction product was an oil.

(45) Samuel, E.; Raush, M. D. *J. Am. Chem. Soc.* **1973**, *95*, 6263.
(46) Jeener, J.; Meier, B. H.; Bachmann, P.; Ernst, R. R. *J. Chem. Phys.* **1979**, *71*, 4546.
(47) Wagner, R.; Berger, S. *J. Magn. Reson. A* **1996**, *123*, 119.
(48) Lix, B.; Sönnichsen, F. D.; Sykes, B. D. *J. Magn. Reson. A* **1996**, *121*, 83.

^{1}H NMR (400.13 MHz, benzene-d_6, 297 K, J in Hz): δ 5.26 (s, Cp^d), 5.24 (s, Cp^u), 2.43 (m, NCH$_2^b$), 2.04 (m, NCH$_2^a$), 1.90 (s, NMe), 1.68 (d $^2J_{H_u-H_d}$ = 8.43, ZrCH$_2^d$), 1.37 (d, $^2J_{H_u-H_d}$ = 8.43 Hz, ZrCH$_2^u$), 1.30−1.39 (b, chain), 0.92 (brt, $^3J_{H_\omega-H_{\omega-1}}$ = 7.05, ωMe), 0.07 (br s, BMe). ^{13}C{^{1}H} NMR (100.55 MHz, benzene-d_6, 297 K): δ 110.3 (Cp^u), 110.2 (Cp^d), 64.8 (NCH$_2$), 55.4 (ZrCH$_2$), 49.0 (NMe), 14.1 (ωMe), −8.4 (BMe). ^{19}F NMR (376.65 MHz, benzene-d_6, 297 K, J in Hz): δ −132.9 (br d, $^3J_{oF-mF}$ = 22.3, *o*-*F*), −160.9 (t, $^3J_{pF-mF}$ = 20.7, *p*-*F*), −165.3 (m, *m*-*F*).

[Cp$_2$Zr(η^2-CH$_2$N(C$_{18}$H$_{37}$)$_2$)$^+\cdots$MeB(C$_6$F$_5$)$_3^-$] (Zr^{NC18}BN). In the glovebox, **Zr^{Me}BN** (20 mg, 26.1 mmol) and NMe(C$_{18}$H$_{37}$)$_2$ (14 mg, 26.1 mmol) were loaded into a J. Young NMR tube and dissolved in approximately 0.7 mL of benzene-d_6. After 2 h, the reaction product was obtained. This compound is soluble in pentane; consequently it was not further purified.

^{1}H NMR (400.13 MHz, benzene-d_6, 297 K, J in Hz) δ 5.43 (s, Cp), 2.43 (m, NCH$_2$), 1.82 (s, ZrCH$_2$), 1.07−1.43 (b, chains), 0.93 (brt, $^3J_{H_\omega-H_{\omega-1}}$ = 7.0, ωMe), 0.25 (br s, BMe). ^{13}C{^{1}H} NMR (100.55 MHz, benzene-d_6, 297 K): δ 111.0 (Cp), 60.8 (NCH$_2$), 56.6 (ZrCH$_2$), 14.5 (ωMe), −5.4 (BMe). ^{19}F NMR (376.65 MHz, benzene-d_6, 297 K, J in Hz): δ −132.7 (br d, $^3J_{oF-mF}$ = 21.2, *o*-*F*), −161.3 (t, $^3J_{pF-mF}$ = 20.8, *p*-*F*), −165.6 (m, *m*-*F*).

[Cp$_2$Zr(η^2-CH$_2$NMe(C$_6$H$_5$))$^+\cdots$MeB(C$_6$F$_5$)$_3^-$] (Zr^{NPh}BN). In the glovebox, 25 mg of **Zr^{Me}BN** (0.033 mmol) was loaded into a J. Young NMR tube and dissolved in approximately 0.7 mL of benzene. With a micrometric syringe, 1.2 equiv of *N*,*N*-dimethylaniline (~5 μL) was added and the mixture was vigorously shaken. The solution immediately became dark yellow, and gas evolution was observed. After a few minutes, a denser oily phase settled to the bottom of the tube. The supernatant solution was removed, the oil was rinsed with benzene (3 × 1 mL), and fresh benzene was added. After 5 h the tube was interfaced to the high-vacuum line and the solvent was removed. The resultant residue was rinsed with pentane (3 × 1 mL) and dried again. The reaction product was an oil.

^{1}H NMR (400.13 MHz, benzene-d_6, 297 K, J in Hz): δ 7.01 (m, *m*-H), 6.82 (br d, $^3J_{oH-mH}$ = 7.9, *o*-H), 6.78 (m, *p*-H), 5.37 (s, Cp^u), 5.10 (s, Cp^d), 2.70 (d, $^2J_{H_u-H_d}$ = 8.8, ZrCH$_2^d$), 2.25 (s, NCH$_3$), 1.75 (d, $^2J_{H_u-H_d}$ = 8.8, ZrCH$_2^u$), 0.41 (br d, BMe). ^{13}C{^{1}H} NMR (100.55 MHz, benzene-d_6, 297 K): δ 156.5 (ipso-C), 129.7 (*m*-C), 127.4 (*p*-C), 121.5 (*o*-C), 111.5 (Cp^d), 111.1 (Cp^u), 57.8 (NMe), 55.6 (ZrCH$_2$), −5.5 (BMe). ^{19}F NMR (376.65 MHz, benzene-d_6, 297 K, J in Hz): δ −132.7 (d $^3J_{oF-mF}$ = 21.8, *o*-F), −161.0 (t $^3J_{pF-mF}$ = 20.8, *p*-F), −165.8 (m, *m*-F).

[Cp$_2$Zr(η^2-CH$_2$NMe(C$_6$H$_5$))$^+\cdots$B(C$_6$F$_5$)$_4^-$] (Zr^{NPh}BT). In the glovebox, 20 mg of **Zr^{Me_2}** (0.0785 mmol) and a stoichiometric amount of HNMe$_2$C$_6$H$_5^+$B(C$_6$F$_5$)$_4^-$ (63 mg) were loaded into a J. Young NMR tube and dissolved in approximately 0.7 mL of benzene-d_6. The mixture was vigorously shaken, and in a few minutes a red dense oily phase settled to the bottom of the tube. Gas evolution was observed. The supernatant solution was removed, and the oil was rinsed with benzene (3 × 1 mL). After 5 h, the tube was interfaced to the high-vacuum line and the solvent was removed. A 3.5 mM solution of **Zr^{NPh}BT** in benzene-d_6 showed no sign of decomposition after 7 days.

^{1}H NMR (400.13 MHz, benzene-d_6/*o*-difluorobenzene 10:1, 297 K, J in Hz): δ 7.18 (m, *m*-H), 7.08 (t, $^3J_{mH-pH}$ = 7.3, *p*-H), 6.88 (d, $^3J_{oH-mH}$ = 7.7, *o*-H), 5.75 (s, Cp^u), 5.46 (s, Cp^d), 3.22 (d, $^2J_{H_u-H_d}$ = 8.8 Hz, ZrCH$_2^d$), 2.62 (s, NMe), 2.48 (d, $^2J_{H_u-H_d}$ = 8.8, ZrCH$_2^u$). ^{13}C{^{1}H} NMR (100.55 MHz, benzene-d_6/*o*-difluorobenzene 10:1, 297 K): δ 156.4 (ipso-C), 130.6 (*m*-C), 128.1 (*p*-C), 121.6 (*o*-C), 113.5 (Cp^d), 113.05 (Cp^u), 60.0 (ZrCH$_2$), 57.79 (NMe). ^{19}F NMR (376.65 MHz, benzene-d_6/*o*-difluorobenzene 10:1, 297 K, J in Hz): δ −131.98 (br d, *o*-F), −162.66 (t, $^3J_{pF-mF}$ = 20.8, *p*-F), −168.23 (m, *m*-F).

[Cp$_2$Zr(η^2-CH$_2$N(C$_{18}$H$_{37}$)$_2$)$^+\cdots$B(C$_6$F$_5$)$_4^-$] (Zr^{NC18}BT). A 20 mg portion of **Zr^{Me_2}** (0.079 mmol) and 0.95 equiv of CPh$_3^+$B(C$_6$F$_5$)$_4^-$ were loaded into a J. Young NMR tube and dissolved in approximately 0.7 mL of chlorobenzene-d_5. The obtained red solution was added to a solution of 1.2 equiv of NMe(C$_{18}$H$_{37}$)$_2$ (51.2 mg) in benzene-d_6, and immediately the color changed to yellow and gas evolution was observed. After 5 h, the J. Young tube was interfaced to the high-vacuum line and the mixture of solvents was removed. The resultant residue was rinsed with pentane (3 × 1 mL) and dried for 2 h. The reaction product was oily. A 42 mM solution of **Zr^{NC18}BT** in benzene-d_6 showed only marginal signs of decomposition in 48 h.

^{1}H NMR (400.13 MHz, benzene-d_6, 297 K): δ 5.58 (s, Cp), 2.65 (m, NCH$_2^a$), 2.50 (m, NCH$_2^b$), 2.61 (s, ZrCH$_2$), 1.55−1.01 (b, chains), 0.93 (br t, ωMe). ^{13}C{^{1}H} NMR (100.55 MHz, 297 K): δ 112.3 (Cp), 61.6 (ZrCH$_2$), 60.2 (NCH$_2$), 14.1 (ωMe). ^{19}F NMR (376.65 MHz, benzene-d_6, 297 K, J in Hz): δ −131.9 (br d, *o*-F), −162.3 (t, $^3J_{pF-mF}$ = 20.8, *p*-F), −167.4 (m, *m*-F).

[Cp$_2$Zr(η^2-CH$_2$NMeEt)(THF)][MeB(C$_6$F$_5$)$_3$] ([Zr^{NC2}THF][BN]). A J. Young NMR tube with a solution of **Zr^{NC2}BN** in approximately 0.7 mL of benzene-d_6 was connected to the high-vacuum line, and an excess of THF was condensed under vacuum at −78 °C into the tube. Immediately, a brightening of the solution was observed. The solvent mixture THF/benzene-d_6 was removed in vacuo. The resultant residue was rinsed with pentane (3 × 1 mL) and dried. The reaction product was an oil. A 0.23 mM solution of **[Zr^{NC2}THF][BN]** in benzene-d_6 is stable at least for 1 week.

^{1}H NMR (400.13 MHz, benzene-d_6, 297 K, J in Hz): δ 5.21 (s, Cp^u), 5.16 (s, Cp^d), 3.04 (m, αTHF), 2.16 (m, NCH$_2^b$), 1.87 (m, NCH$_2^a$), 1.78 (s, NMe), 1.68 (d, $^2J_{H_u-H_d}$ = 8.6, ZrCH$_2^d$), 1.38 (m, βTHF), 1.32 (br s, BMe), 1.31 (d, $^2J_{H_u-H_d}$ = 8.6, ZrCH$_2^u$), 0.74 (brt, $^3J_{H_\omega-NCH_2}$ = 6.96, ωMe). ^{13}C{^{1}H} NMR (100.55 MHz, benzene-d_6, 297 K): δ 110.6 (Cp^u), 110.5 (Cp^d), 78.2 (NCH$_2$), 77.6 (αTHF), 59.4 (ZrCH$_2$), 49.6 (NMe), 25.8 (βTHF), 9.4 (ωMe). ^{19}F NMR (376.65 MHz, benzene-d_6, 297 K, J in Hz): δ −132.3 (br d, $^3J_{oF-mF}$ = 20.0, *o*-*F*), −164.5 (t, $^3J_{pF-mF}$ = 20.7, *p*-*F*), −167.1 (m, *m*-*F*).

[Cp$_2$Zr(η^2-CH$_2$NMe(C$_{16}$H$_{33}$))(THF)][MeB(C$_6$F$_5$)$_3$] ([Zr^{NC16}THF][BN]). A J. Young NMR tube with a solution of **Zr^{NC16}BN** in approximately 0.7 mL of benzene was connected to the high-vacuum line, and an excess of THF was condensed in. A brightening of the solution was observed. The mixture of solvents was removed in vacuo. The resultant residue was rinsed with pentane (3 × 1 mL) and finally dried. The product was an oil. An 8.45 mM solution of **[Zr^{NC16}THF][BN]** in benzene-d_6 is stable at least for 1 month.

^{1}H NMR (400.13 MHz, benzene-d_6, 297 K, J in Hz): δ 5.28 (s, Cp^u), 5.26 (s, Cp^d), 3.10 (m, αTHF), 2.30 (m, NCH$_2^b$), 2.03 (m, NCH$_2^a$), 1.92 (s, NMe), 1.87 (d, $^2J_{H_u-H_d}$ = 8.92, ZrCH$_2^d$), 1.49 (d, $^2J_{H_u-H_d}$ = 8.92, ZrCH$_2^u$), 1.37−1.43 (b, chain), 1.37 (b, βTHF), 1.32 (br s, BMe), 0.94 (br t, $^3J_{H_\omega-H_{\omega-1}}$ = 6.97, ωMe). ^{13}C{^{1}H} NMR (100.55 MHz, benzene-d_6, 297 K): δ 110.3 (Cp^u), 110.0 (Cp^d), 77.6 (αTHF), 65.1 (NCH$_2$), 55.1 (ZrCH$_2$), 49.6 (NMe), 25.8 (βTHF), 14.5 (ωMe), 11.5 (BMe). ^{19}F NMR (376.65 MHz, benzene-d_6, 297 K, J in Hz): δ −132.2 (br d, $^3J_{oF-mF}$ = 23.3, *o*-*F*), −164.4 (t, $^3J_{mF-pF}$ = 20.8, *p*-*F*), −167.0 (m, *m*-*F*).

[Cp$_2$Zr(η^2-CH$_2$N(C$_{18}$H$_{37}$)$_2$)(THF)][MeB(C$_6$F$_5$)$_3$] ([Zr^{NC18}THF][BN]). In the glovebox, into a J. Young NMR tube, a solution of **Zr^{NC18}BN** in approximately 0.7 mL of benzene-d_6 was prepared using a slight excess of NMe(C$_{18}$H$_{37}$)$_2$ (5%). The tube was interfaced to the high-vacuum line, and an excess of THF was condensed in at −78 °C. Then the solvent was removed in vacuo. The resultant oily residue was rinsed with pentane (3 × 1 mL) and dried.

^{1}H NMR (400.13 MHz, benzene-d_6, 297 K, J in Hz): δ 5.39 (s, Cp), 3.2 (m, αTHF), 2.39 (m, NCH$_2$), 1.88 (s, ZrCH$_2$), 1.36 (s, βTHF), 1.33 (br s, BMe), 1.10−1.50 (b, chains), 0.95 (br t, $^3J_{H_\omega-H_{\omega-1}}$ = 7.0, ωMe). ^{13}C{^{1}H} NMR (100.55 MHz, benzene-d_6,

297 K): δ 111.3 (Cp), 78.0 (αTHF), 62.2 ($ZrCH_2$), 53.8 (NCH_2), 25.4 (βTHF), 14.7 (ωMe), 12.4 (BMe). ^{19}F NMR (376.65 MHz, benzene-d_6, 297 K, J in Hz): δ −132.3 (br d, $^3J_{oF-mF}$ = 20.3, *o*-*F*), −164.4 (t, $^3J_{mF-pF}$ = 20.8, *p*-*F*), −167.0 (m, *m*-*F*).

[$Cp_2Zr(\eta^2$-$CH_2NMe(C_6H_5))(THF)][MeB(C_6F_5)_3]$ ([Zr^{NPh}THF]-[BN]). A J. Young NMR tube containing a solution of **Zr^{NPh}BN** in benzene-d_6 was interfaced to the high-vacuum line, and an excess of THF was condensed in at −78 °C. The solution immediately changed from dark to bright yellow. The mixture of solvents was quickly removed in vacuo, and the residue was rinsed with pentane (3 × 1 mL) and dried. The reaction product was an oil.

^1H NMR (400.13 MHz, benzene-d_6/chlorobenzene-d_5 1:1, 297 K, J in Hz): δ 7.11 (m, *m*-H), 6.99 (t, $^3J_{pH-mH}$ = 7.7, *p*-H), 6.74 (d, $^2J_{oH-mH}$ = 7.7, *o*-H), 5.39 (s, Cp^u), 5.10 (s, Cp^d), 3.28 (m, αTHF), 2.56 (d, $^2J_{H_u-H_d}$ = 7.9, $ZrCH_2{}^d$), 2.27 (s, NMe), 2.15 (d, $^2J_{H_u-H_d}$ = 7.9, $ZrCH_2{}^u$), 1.46 (m, βTHF), 1.27 (br d, BMe). $^{13}C\{^1H\}$ NMR (100.55 MHz, benzene-d_6/chlorobenzene-d_5 1:1, 297 K): δ 156.7 (ipso-C), 129.9 (*m*-C), 128.1 (*p*-C), 123.4 (*o*-C), 110.6 (Cp^d), 109.6 (Cp^u), 77.5 (αTHF), 59.0 (NMe), 57.6 ($ZrCH_2$), 25.5 (βTHF), 11.2 (ωMe). ^{19}F NMR (376.65 MHz, benzene-d_6/chlorobenzene-d_5 1:1, 297 K, J in Hz): δ −132.3 (d, $^3J_{oF-mF}$ = 21.8, *o*-F), −164.3 (t, $^3J_{pF-mF}$ = 20.8, *p*-F), −166.9 (br d, *m*-F).

[$Cp_2Zr(\eta^2$-$CH_2NMe(C_6H_5))(THF)][B(C_6F_5)_4]$ ([Zr^{NPh}THF]-[BT]). A J. Young NMR tube containing a solution of **Zr^{NPh}BT** in benzene-d_6/chlorobenzene-d_5 was interfaced to the high-vacuum line, and an excess of THF was condensed under vacuum at −78 °C. The mixture of solvents was removed in vacuo, and the resultant residue was rinsed with pentane (3 × 1 mL) and dried again.

^1H NMR (400.13 MHz, benzene-d_6/chlorobenzene-d_5 1:1, 297 K, J in Hz): δ 7.10 (m, *m*-H), 7.02 (t $^3J_{pH-mH}$ = 7.3, *p*-H), 6.77 (d, $^2J_{oH-mH}$ = 7.7, 2H, *o*-H), 5.43 (s, Cp^u), 5.13 (s, Cp^d), 3.33 (m, α THF), 2.61 (d, $^2J_{H_u-H_d}$ = 8.3, $ZrCH_2{}^d$), 2.31 (s, NMe), 2.19 (d, $^2J_{H_u-H_d}$ = 8.3, $ZrCH_2{}^u$), 1.49 (m, βTHF). $^{13}C\{^1H\}$ NMR (400 MHz, benzene-d_6/chlorobenzene-d_5 1:1, 297 K): δ 156.7 (ipso-C), 129.7 (*m*-C), 127.5 (*p*-C), 123.0 (*o*-C), 110.3 (Cp^d), 109.3 (Cp^u), 77.2 (αTHF), 58.7 (NMe), 57.4 ($ZrCH_2$), 25.3 (βTHF). ^{19}F NMR (376.65 MHz, benzene-d_6/chlorobenzene-d_5 1:1, 297 K, J in Hz): δ −132.5 (br d, *o*-F), −162.7 (t, $^3J_{oF-pF}$ = 20.8, *p*-F), −166.7 (m, *m*-F).

[$Cp_2Zr(\eta^2$-$CH_2N(C_{18}H_{37})_2)(THF)][B(C_6F_5)_4]$ ([Zr^{NC18}THF]-[BT]). A J. Young NMR tube containing a solution of **Zr^{NC18}BT** in benzene-d_6/chlorobenzene-d_5 was interfaced to the high-vacuum line, and an excess of dry THF was condensed in at −78 °C. A brightening of the solution was observed. Then, the mixture of solvents was removed in vacuo and the resultant residue was dried for 2 h. The reaction product was oily.

^1H NMR (400 MHz, benzene-d_6, 297 K): δ 5.38 (s, Cp), 3.19 (m, αTHF), 2.39 (m, NCH_2), 1.88 (s, $ZrCH_2$), 1.6−1.0 (b, chains/βTHF), 0.94 (br t, ωMe). $^{13}C\{^1H\}$ NMR (100.55 MHz, benzene-d_6, 297 K): δ 110.1 (Cp), 77.3 (α), 61.6 ($ZrCH_2$), 60.2 (NCH_2), 14.1 (ωMe). ^{19}F NMR (376.65 MHz, benzene-d_6, 297 K, J in Hz): δ −132.2 (br d, *o*-F), −162.5 (t, $^3J_{mF-pF}$ = 20.8 Hz, *p*-F), −166.5 (m, *m*-F).

PGSE Measurements. ^1H and ^{19}F PGSE NMR measurements were performed by using the standard stimulated echo pulse sequence on a Bruker AVANCE DRX 400 spectrometer equipped with a GREAT 1/10 gradient unit and a QNP probe with a Z-gradient coil, at 297 K without spinning. The dependence of the resonance intensity (I) on a constant waiting time and on a varied gradient strength (G) is described by the equation

$$\ln \frac{I}{I_0} = -(\gamma\delta)^2 D_t \left(\Delta - \frac{\delta}{3}\right) G^2$$

where I = intensity of the observed spin echo, I_0 = intensity of the spin echo in the absence of a gradient, D_t = self-diffusion coefficient, Δ = delay between the midpoints of the gradients, δ = length of the gradient pulse, and γ = magnetogyric ratio. The shape of the gradients was rectangular, their lengths δ were 4−5 ms, and their strengths G were varied during the experiments. All spectra were acquired using 32K points and a spectral width of 5000 (^1H) and 18 000 (^{19}F) Hz, and they were processed with a line broadening of 1.0 (^1H) and 1.5 (^{19}F). The semilogarithmic plots of $\ln(I/I_0)$ versus G^2 were fitted using a standard linear regression algorithm, and a correlation factor better than 0.99 was always obtained. Different values of Δ, G, and numbers of transients were used for different samples.

The self-diffusion coefficient D_t, which is directly proportional to the slope (m) of the regression line obtained by plotting $\ln(I/I_0)$ versus G^2, was estimated by evaluating the proportionality constant using a sample of HDO (5%) in D_2O (known diffusion coefficients in the range 274−318 K)[49] under the same exact conditions as for the sample of interest. The solvent was taken as an internal standard. D_t data were treated as described in the literature in order to derive the hydrodynamic dimensions.[36d,39,50] The measurement uncertainty was estimated by determining the standard deviation of m when performing experiments with different Δ values. Error propagation analysis yielded a standard deviation of approximately 3−4% in the hydrodynamic radius and 10−15% in the aggregation number N. NMR samples for PGSE NMR measurements were prepared inside the glovebox by successive dilutions. The actual concentration was estimated from integration relative to an external standard.

Computational Details. Density fuctional calculation were performed with the Turbomole program[51] (version 5.8) in combination with the OPTIMIZE routine of Baker and coworkers.[52] All geometries were fully optimized at the B3LYP level,[53] using the single-ζ SV(P)[54] basis set (small-core pseudopotential on Zr[55]). All the structures were characterized by vibrational analyses using analytic or numerical second derivatives, in order to check that no imaginary frequencies were present. Improved electronic energies were calculated at the SV(P) optimized geometries using the TZVP basis set on all atoms.[56] Single-point solvent corrections were calculated using the conductor-like screening model (COSMO)[57] with ε_r = 2.3 to model an apolar solvent. If not otherwise noted, all the

(49) (a) Tyrrell, H. J. W.; Harris, K. R. *Diffusion in Liquids*; Butterworth: London, 1984. (b) Mills, R. *J. Phys. Chem.* **1973**, *77*, 685.

(50) Cabrita, E. J.; Berger, S. *Magn. Reson. Chem.* **2001**, *39*, S142.

(51) (a) Ahlrichs, R.; Bär, M.; Baron, H.-P.; Bauernschmitt, R.; Böcker, S.; Ehrig, M.; Eichkorn, K.; Elliott, S.; Furche, F.; Haase, F.; Häser, M.; Hättig, C.; Horn, H.; Huber, C.; Huniar, U.; Kattannek, M.; Köhn, A.; Kölmel, C.; Kollwitz, M.; May, K.; Ochsenfeld, C.; Ohm, H.; Schäfer, A.; Schneider, U.; Treutler, O.; Tsereteli, K.; Unterreiner, B.; von Arnim, M.; Weigend, F.; Weis, P.; Weiss, H. *Turbomole, Version 5*; Theoretical Chemistry Group, University of Karlsruhe, Karlruhe, Germany, 2002. (b) Treutler, O.; Ahlrichs, R. *J. Chem. Phys.* **1995**, *102*, 346.

(52) (a) *PQS, version 2.4*; Parallel Quantum Solutions:, Fayetteville, AK, 2001 (the Baker optimizer is available separately from PQS upon request). (b) Baker, J. *J. Comput. Chem.* **1986**, *7*, 385.

(53) (a) Lee, C.; Yang, W.; Parr, R. G. *Phys. Rev. B* **1988**, *37*, 785. (b) Becke, A. D. *J. Chem. Phys.* **1993**, *98*, 1372. (c) Becke, A. D. *J. Chem. Phys.* **1993**, *98*, 5648. (d) Calculations were performed using the Turbomole functional "b3-lyp", which is not identical with the Gaussian "B3LYP" functional.

(54) Schäfer, A.; Horn, H.; Ahlrichs, R. *J. Chem. Phys.* **1992**, *97*, 2571.

(55) Andrae, D.; Häussermann, U.; Dolg, M.; Stoll, H.; Preuss, H. *Theor. Chim. Acta* **1990**, *77*, 123.

(56) Schäfer, A.; Huber, C.; Ahlrichs, R. *J. Chem. Phys.* **1994**, *100*, 5829.

(57) Schäfer, A.; Klamt, A.; Sattel, D.; Lohrenz, J. C. W.; Eckert, F. *Phys. Chem. Chem. Phys.* **2000**, *2*, 2187.

energies are calculated with solvation correction. Initial geometries and reasonable starting Hessians were obtained from PM3 computations with the Spartan package from Wavefunction Inc.[58]

(58) Shao, Y.; Molnar, L. F.; Jung, Y.; Kussmann, J.; Ochsenfeld, C.; Brown, S. T.; Gilbert, A. T. B.; Slipchenko, L. V.; Levchenko, S. V.; O'Neill, D. P.; DiStasio, R. A., Jr.; Lochan, R. C.; Wang, T.; Beran, G. J. O.; Besley, N. A.; Herbert, J. M.; Lin, C. Y.; Van Voorhis, T.; Chien, S. H.; Sodt, A.; Steele, R. P.; Rassolov, V. A.; Maslen, P. E.; Korambath, P. P.; Adamson, R. D.; Austin, B.; Baker, J.; Byrd, E. F. C.; Dachsel, H.; Doerksen, R. J.; Dreuw, A.; Dunietz, B. D.; Dutoi, A. D.; Furlani, T. R.; Gwaltney, S. R.; Heyden, A.; Hirata, S.; Hsu, C.-P.; Kedziora, G.; Khalliulin, R. Z.; Klunzinger, P.; Lee, A. M.; Lee, M. S.; Liang, W. Z.; Lotan, I.; Nair, N.; Peters, B.; Proynov, E. I.; Pieniazek, P. A.; Rhee, Y. M.; Ritchie, J.; Rosta, E.; Sherrill, C. D.; Simmonett, A. C.; Subotnik, J. E.; Woodcock, H. L., III; Zhang, W.; Bell, A. T.; Chakraborty, A. K.; Chipman, D. M.; Keil, F. J.; Warshel, A.; Hehre, W. J.; Schaefer, H. F.; Kong, J.; Krylov, A. I.; Gill, P. M. W.; Head-Gordon, M. *Phys. Chem. Chem. Phys.* **2006**, *8*, 3172.

Acknowledgment. This work was supported by grants from the Ministero dell'Istruzione, dell'Università e della Ricerca through the PRIN 2007 (2007X2RLL2) program. We thank Prof. Giuseppe Cardaci for helpful discussions.

Supporting Information Available: Figures and tables giving selected PGSE NMR data in benzene-d_6 and cyclohexane-d_{12} and additional structures of the complexes. This material is available free of charge via the Internet at http://pubs.acs.org.